

# Advances and New Challenges to Bimolecular Reaction Dynamics Theory

Jun Li,\* Bin Zhao,\* Daiqian Xie,\* and Hua Guo\*

Cite This: *J. Phys. Chem. Lett.* 2020, 11, 8844–8860

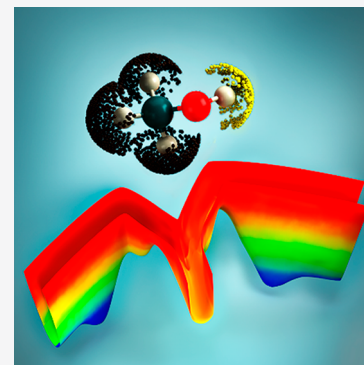
Read Online

ACCESS |

Metrics &amp; More

Article Recommendations

**ABSTRACT:** Dynamics of bimolecular reactions in the gas phase are of foundational importance in combustion, atmospheric chemistry, interstellar chemistry, and plasma chemistry. These collision-induced chemical transformations are a sensitive probe of the underlying potential energy surface(s). Despite tremendous progress in past decades, our understanding is still not complete. In this Perspective, we survey the recent advances in theoretical characterization of bimolecular reaction dynamics, stimulated by new experimental observations, and identify key new challenges.



Chemical processes in the gas phase are of great importance in a number of environments, such as combustion, plasmas, atmospheres, and interstellar clouds. In the absence of condensed media, the breaking and forming of chemical bonds in a bimolecular reaction require collisions, thus providing an ideal probe of the interaction potential within and between the collision partners, without any interference from solvent or other solute molecules. It has long been recognized that reactivity of a gaseous reaction depends on not only the total energy for overcoming the reaction barrier but also many other factors such as the impact parameter, attacking angles, orientation and/or alignment of reactants, and the energy content/type of the reactants.<sup>1</sup> A complete understanding of reaction dynamics requires the delineation of all factors that influence the reactivity, which is difficult to achieve under thermal conditions. Our current knowledge of chemical reactivity is strongly influenced by the revolution initiated by crossed molecular beams<sup>2</sup> and laser technology,<sup>3</sup> which allow the preparation of well-defined initial translational and internal energies of reactants. Probing product energy disposal with quantum state resolution completes the circle, providing state-to-state information on collisions and chemical transformation.

In recent years, experimental advances have greatly improved our ability to ask more detailed questions about chemical dynamics. On one hand, molecular beam and laser techniques are now routinely utilized to prepare a single ro-vibrational quantum state and align or orient molecules before collision.<sup>4–6</sup> On the other hand, techniques, such as Rydberg tagging and velocity map imaging, have greatly advanced our ability to accurately measure product quantum states and branching ratios.<sup>4,7,8</sup> Cooling molecules or controlling the collisional

velocity allows a reduction of partial waves, significantly decreasing averaging over the impact parameter.<sup>5,9,10</sup> Indeed, ultracold collisions rely on a single partial wave and are completely dominated by quantum effects.<sup>11</sup> These advances have revealed many interesting phenomena concerning reaction dynamics, including mode specificity, bond selectivity, product branching and internal excitations, tunneling and resonances, stereodynamics, and nonadiabatic effects. They challenge theory to provide insights into chemical reactivity in an unprecedented range of reaction conditions.<sup>7,8,11–14</sup>

Except for complex-forming reactions, it is generally difficult to probe directly the dynamics in the strongly interacting region of a reactive process, because of the fleeting nature of the transition state. The aforementioned experimental asymptotic approaches do not reveal how exactly a chemical reaction takes place. To this end, theoretical studies become a necessity for gaining insight into reaction dynamics and to ultimately control chemical reactivity, by offering intimate details of the chemical dynamics and by providing intuitive mechanistic models.<sup>15–17</sup> In most chemical processes, nuclear dynamics is governed by the Born–Oppenheimer potential energy surface (BO PES), which gives rise to the forces acting on the nuclei. This intuitive picture of nuclear motion on a multidimensional PES benefits from the

Received: August 16, 2020

Accepted: September 24, 2020

Published: September 24, 2020

natural separation of the electronic motion from that of nuclei, although it can break down near electronic degeneracies.<sup>18</sup> Recent advances in both electronic structure theory and fitting techniques have perfected our ability to map out global PESs with high accuracy and efficiency for not just simple A + BC type reactions, but also for systems involving many nuclear degrees of freedom (DOFs).<sup>19–24</sup> These advances enabled quantum and classical investigations of scattering dynamics of polyatomic reactions,<sup>17,25–30</sup> which might have multiple channels leading to different products. Direct dynamics studies, which compute the forces on the fly without analytical PESs, provide an alternative means to explore chemical dynamics in even larger systems.<sup>31</sup> However, such on-the-fly calculations are generally limited to fast processes and often are done at low levels of electronic structure theory. In addition, they cannot be used for quantum dynamical computations because of the nonlocal nature of the scattering wave function.

In this Perspective, we survey recent advances in theoretical characterization of reaction dynamics of gas-phase bimolecular reactions and identify new challenges and opportunities. We will focus on the latest developments since the last comprehensive review of the field in 2016.<sup>17</sup> While theoretical studies of reaction kinetics are closely related to issues discussed here, they are not extensively discussed in this Perspective. Furthermore, we will restrict our attention to reactions involving two reactants.

The BO PES is a fundamental concept in chemistry. Most theoretical investigations on spectroscopy, kinetics, and dynamics require the underlying PES of the system. The accuracy and efficiency of the PES are the key factors that determine the reliability of dynamical outcome and costs of the dynamical computations. Most current PESs<sup>20,21,28,32</sup> are based on high-level *ab initio* electronic structure theories, such as coupled cluster singles, doubles, and perturbative triples (CCSD(T))<sup>33</sup> and multireference configuration interaction (MRCI) methods,<sup>34</sup> which account for electron correlation, and their F12 variants.<sup>35</sup> Interestingly, some density functional theory-based PESs reported recently have shown promise to rival high-level theories at significantly less computational costs,<sup>36,37</sup> but their general applicability still needs further confirmation. Unlike nonreactive systems, reactions involve bond breaking and forming, which are often accompanied by significant changes in the electronic structure. This might lead to failure of single-reference treatments such as CCSD(T). For example, CCSD(T) breaks down in certain regions of the PES for the OH<sup>-</sup> + CH<sub>3</sub>I reaction, resulting in unphysically large reaction cross sections.<sup>38</sup> MRCI calculations for such a system are too expensive and not affordable currently, and thus alternative approaches are needed. Even when CCSD(T) is generally amenable, convergence to the correct state can sometimes be difficult in the presence of low-lying excited states. In the prototypical radical–radical reaction OH + HO<sub>2</sub> → H<sub>2</sub>O + O<sub>2</sub>, for example, correct convergence to the ground state by CCSD(T), which is efficient and accurate, can be achieved only by using appropriate Hartree–Fock initial guesses.<sup>39</sup> Further improvements of the *ab initio* calculations can be achieved by considering extrapolating energies to the complete basis set, higher-order correlations, core-correlation effects, the contributions of the relativistic corrections, spin–orbit corrections, etc.<sup>23,40</sup> While the accuracy of electronic structure theories has improved tremendously in past decades,<sup>41</sup> there is still significant need for new and more efficient theories in treating reactive systems, particularly those with multireference character.

There has been significant progress in high-fidelity representation of high-dimensional PESs based on large numbers of *ab initio* energy points. These can be achieved by using machine learning approaches such as linear<sup>21,28</sup> and kernel-based regression,<sup>42</sup> as well as neural networks (NNs).<sup>20,22,43</sup> A PES should be invariant under the complete nuclear permutation and inversion (CNPI) group,<sup>44</sup> which is important for calculating spectra and dynamics of molecular systems that contain identical nuclei. There are several approaches to enforce the permutation symmetry, including the permutationally invariant polynomials (PIPs),<sup>19,21</sup> PIP-neural network (PIP-NN),<sup>20</sup> fundamental invariant-NN (FI-NN),<sup>22</sup> atomistic NN (AtNN),<sup>43</sup> and kernel-based methods using permutationally invariant descriptors.<sup>45</sup> The representation of PESs and symmetry adaption have been extensively considered in recent reviews<sup>21,46</sup> and thus are not discussed in detail here. We note that such techniques have led to accurate reactive PESs for large (up to nine atoms) systems with multiple product arrangement channels,<sup>47–57</sup> allowing dynamic investigations of not just overall reactivity but also detailed information on product branching. An extension based on many-body expansion was recently proposed,<sup>58</sup> which may have some advantages over the fitting of the full PES. A challenge is to extend such high-fidelity representation of PESs to reactive systems with more than 10 atoms, for which some progress has already been made.<sup>54,59,60</sup> To this end, the AtNN method is very attractive because it can in principle be employed for fitting PESs of large polyatomic systems with exact symmetry properties and high fitting accuracy. Alternatively, more approximate strategies can be used.<sup>61–63</sup>

An interesting approach to determining reactive PESs is to extract PES information from scattering attributes using machine learning. Such an inversion approach has been demonstrated recently for a four-atom reaction<sup>64</sup> using multiple quantum scattering calculations. This concept can in principle be used to “observe” PESs based on experimental data.

Another challenge is the construction of diabatic potential energy matrices (DPEMs) for reactive systems beyond the BO approximation because of electronic degeneracies such as conical intersections (CIs).<sup>65,66</sup> Given the discontinuous nature of adiabatic PESs and singularities of the nonadiabatic couplings at CI seams, the adiabatic representation is not appropriate for dynamic calculations,<sup>18,67</sup> despite the fact that all *ab initio* calculations are done in this representation. These problems can be avoided by working in the diabatic representation, in which elements of a DPEM are smooth functions of the nuclear coordinates, as the singular derivative coupling is eliminated or minimized. This diabaticization process via an adiabatic-to-diabatic transformation is however not unique for polyatomic systems,<sup>68,69</sup> and several different strategies exist.<sup>66</sup> As in representing adiabatic PESs, the permutation symmetry needs be properly taken into consideration in constructing DPEMs,<sup>70–74</sup> as demonstrated in the recent work on the X + CH<sub>4</sub> type reactions.<sup>75</sup>

With the PESs, one can perform dynamical calculations using either quantum or classical methods. Quantum dynamic (QD) studies of reactive scattering are currently restricted to low-dimensional systems because of the so-called “dimensionality curse”, namely the fact that the size of the problem (*N*) increases exponentially with the number of DOFs. Time-independent quantum mechanical (TIQM) approaches solve the time-independent Schrödinger equation as a boundary value problem, thus scale steeply with the problem size ( $\propto N^3$ ). It is

well-suited for cold collisions as it can handle very low collision energies. On the other hand, solving the time-dependent Schrödinger equation or its equivalent wave packet (WP) method is an initial value problem, with much better scaling with respect to the problem size ( $\propto N \log N$ ). As a result, most quantum reactive scattering calculations beyond triatomic systems have employed WP methods. The extraction of the  $S$ -matrix is generally difficult, because optimal global coordinates are difficult to find for different arrangement channels. For both reactant and product coordinate-based methods, transformations between two or more coordinates are unavoidable. An alternative solution is provided by the transition state wave packet (TSWP) framework,<sup>76,77</sup> in which initial WPs are prepared in the transition-state region as the eigenstates of a thermal flux operator. Initial state-specific information is extracted by overlapping with asymptotic states after the WPs are propagated to the asymptotic regions. These different state-to-state approaches to overcoming the “coordinate problem” have been extensively discussed in a recent review,<sup>30</sup> supplemented by some further improvements.<sup>78,79</sup> For atom–diatom problems, the hyperspherical coordinates allow three arrangement channels to be treated equally, which is particularly important for  $X_3$  type systems where the three channels are identical. This widely used coordinate system in TIQM treatments has recently been implemented in a WP framework.<sup>80</sup> While it requires six times more basis functions, the computational time increases much slower with the total angular momentum than those using Jacobi coordinates, because of different forms of the Coriolis coupling terms in the kinetic energy operator.

Wave functions as solutions to the Schrödinger equation have to satisfy appropriate boundary conditions. Usually, complex absorbing potential is used to damp WPs before they reach the edges of the grids. For chemical reactions occurring at low temperatures, an extremely long range of absorbing potential is required to damp the long de Broglie wave in the scattering asymptotes. By adding a third long-range region to an  $L$ -shaped representation of a wave function, the part of the wave function in the long-range region can be efficiently propagated within a small subspace of the Hilbert space.<sup>81</sup> This extension renders the WP method feasible for reactions at low collision energies, all the way down to the Wigner threshold regime. Another approach extends the transparent boundary conditions, which were usually used with low-order finite difference methods, to the discrete variable representation.<sup>82</sup> Using one-dimensional models, the transparent boundary conditions were shown to achieve high accuracy in a wide range of translational energy, including those with long de Broglie wavelengths.

Many polyatomic reactions involve some spectator modes. If they can be described by a favorable set of coordinates, the basis/grid required can be significantly reduced. Recently, mixed polyspherical Jacobi and Radau coordinates were used for an efficient description of reaction systems with polyatomic spectator moieties. The spectator moiety can be efficiently described by Radau vectors so that a smaller potential optimized discrete variable representation<sup>83</sup> basis is sufficient for its vibration. This approach has been employed in full-dimensional calculations of initial state selected reaction probabilities for the  $H + NH_3 \rightarrow H_2 + NH_2$  (9D)<sup>84</sup> and the  $H + CH_4 \rightarrow H_2 + CH_3$  (12D) reactions.<sup>85</sup> For the former case, this efficient coordinate system reduces the size of the basis set by more than 85% when compared to a previous study of the same reaction with Jacobi coordinates.

Theoretical studies become a necessity for gaining insight into reaction dynamics and to ultimately control chemical reactivity, by offering intimate details of the chemical dynamics and by providing intuitive mechanistic models.

Further progress has also been achieved using the multi-configuration time-dependent Hartree (MCTDH) approach. Currently, almost all the full-dimensional quantum dynamical studies of the  $H + CH_4 \rightarrow H_2 + CH_3$  reaction rely on the MCTDH approach and its multilayer extension within the quantum transition-state framework. In the coordinate system used in these studies, the body-fixed frame is tied to the methyl fragment based on a 3 + 1 Radau construction. A recent study shows that redefining the methyl-fixed frame reduces the correlation between the methyl rotation and its internal motion and thus results in a smaller basis.<sup>86</sup> Besides the studies of the  $H + CH_4 \rightarrow H_2 + CH_3$  reaction,<sup>87,88</sup> the MCTDH approach has recently been extended to the study of the initial state-selected reaction probabilities<sup>89–91</sup> of the  $H + CHD_3 \rightarrow H_2 + CD_3$  reaction and the quasi-bound states in the prereaction well of the  $F + CH_4 \rightarrow HF + CH_3$  reaction.<sup>92,93</sup> Applications to state-to-state reaction probabilities are forthcoming.

Determination of cross sections is challenging because of the involvement of multiple partial waves. A rigorous transition-state-based rotational sudden (TSRS) method has recently been formulated for calculating integral cross sections (ICSSs).<sup>94</sup> In the TSRS method, eigenvalues and eigenvectors of the rigid rotor Hamiltonian describing the overall rotation of the system at a fixed transition-state geometry are first solved. Reaction probabilities of all partial waves are then approximated by a weighted sum of the reaction probability of  $J = 0$  partial wave after shifting the energy with the corresponding rotational eigenvalues. Differential cross sections (DCSSs) are much harder to compute than ICSSs, but breakthroughs have been made for large reactive systems. Recently, a reduced-dimensional (7D) approach has been successfully applied by Zhang and co-workers to the  $Cl + CH_4$  reaction,<sup>95</sup> based on the Palma–Clary model that fixes the  $C_{3v}$  symmetry of the methyl moiety.<sup>96</sup> This is the first determination of DCSSs in systems with dimensionality greater than six. The TSWP method can in principle be used to determine DCSSs with even higher dimensionalities.<sup>76,97</sup>

Apart from algorithmic developments highlighted above, new ideas on understanding reactive scattering have also been proposed. For example, Manthe and co-workers discussed a decomposition scheme that allows the definition of the so-called natural channels from the  $S$ -matrix elements.<sup>91,98</sup> They can be considered as uniquely defined reaction pathways from reactants and products through the transition state. The corresponding natural reaction probabilities are simply the eigenvalues of the reaction probability operator. This viewpoint offers a rigorous yet intuitive way to think about state-to-state reaction dynamics.

Reactive scattering is also widely investigated using the quasi-classical trajectory (QCT) method, which describes the nuclear dynamics within classical mechanics. The term “quasi-classical” refers to the initial state preparation which enforces the quantization of the reactant internal states.<sup>99</sup> In comparison

The accuracy and efficiency of the PES are the key factors that determine the reliability of the dynamical outcome and costs of the dynamical computations.

with QD methods, QCT is intuitive, numerically inexpensive, and often provides reasonably accurate dynamical information, particularly when the attributes are highly averaged. A major deficiency of QCT is its inability to treat quantum effects such as tunneling and zero-point energy (ZPE). It also tends to overestimate energy flow among different internal DOFs. Recently, there have been some exciting developments in mitigating these deficiencies while retaining the attractive features. In QCT, the standard method for sampling the initial reactant ro-vibrational quantum states is generally based on normal mode approximation, which might provide a nonstationary ensemble because the real PESs are anharmonic. Therefore, uncertainties are introduced in the calculated dynamics. Adiabatic switching can mitigate this problem for polyatomic species.<sup>100,101</sup> A popular approach in determining the product vibrational distributions is to use a Gaussian function in binning the vibrational quantum numbers,<sup>102</sup> which removes the ZPE violating trajectories and often improves the results. The Gaussian binning method can be quite demanding for low-probability channels, so modifications have been proposed.<sup>103,104</sup> Further, ZPE violation can be avoided by running the dynamics on a ZPE-corrected PES.<sup>105</sup> More recently, efforts have been made to take advantage of semiclassical ideas such as the ring-polymer molecular dynamics

(RPMD).<sup>106</sup> RPMD takes advantage of the isomorphism between the statistical properties of a quantum system and those of fictitious harmonically connected classical beads, which allows the computation of quantum attributes using classical trajectories. In some special cases, RPMD provides exactly the same results as quantum mechanics. The original RPMD ansatz was based on Boltzmann statistics and thus is applicable only to thermal conditions.<sup>107,108</sup> Indeed, RPMD has been successfully used to compute thermal rate coefficients for bimolecular reactions and shown to effectively capture the ZPE, anharmonicity, and tunneling with reasonable accuracy.<sup>109,110</sup> More recently, it has been extended to study collisional dynamics under both thermal<sup>111</sup> and microcanonical conditions.<sup>112,113</sup> Preliminary results have been quite encouraging, although no rigorous justification has been provided for these *ad hoc* applications. More investigations are needed to explain its apparent success. Finally, we note in passing that QCT can also be calculated on the fly, without an analytical PES.<sup>31</sup> Despite their superior ability in exploring mechanistic issues, however, such calculations are often performed with relatively low levels of electronic structure theory, and the number of trajectories is often too small to provide quantitatively accurate statistics.

Dynamical calculations on PESs yield many important experimentally observable attributes. Mode specificity is referred to the differing reactivity resulted from exciting different reactant modes. Evidence of mode specificity in bimolecular reactions, which has been known for some time,<sup>114</sup> underscores the dynamic nature of activated reactions. Polanyi rationalized the mode specificity in atom–diatom reactions by the location of the transition state: translational excitation is more effective in promoting an early barrier reaction while vibrational excitation is more effective in promoting a late barrier reaction.<sup>115</sup> These

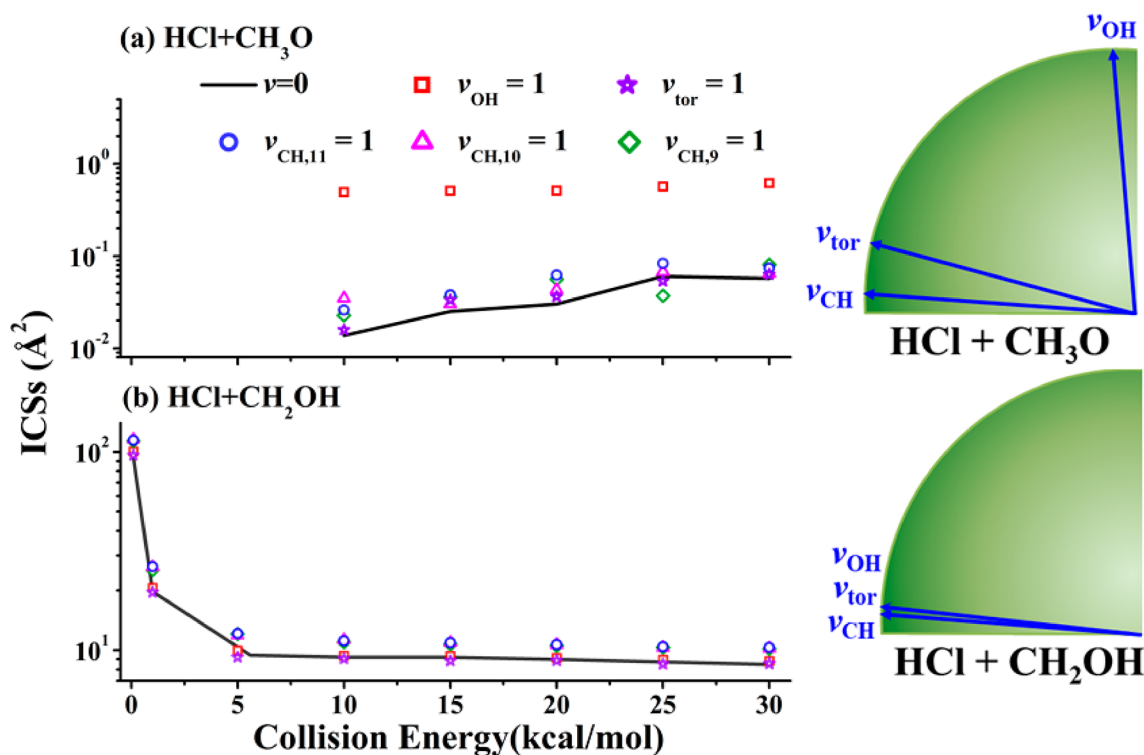


**Figure 1.** Calculated reactive integral cross sections of the reaction  $\text{Cl} + \text{CH}_3\text{OH} \rightarrow \text{HCl} + \text{CH}_3\text{O}/\text{CH}_2\text{OH}$  as a function of the collision energy  $E_c$  (in  $\text{kcal mol}^{-1}$ ) from different initial conditions. The SVP predictions of the relevant modes are also shown. Modified from ref 55 with permission. Copyright 2020 American Chemical Society.

Polanyi rules have been extended to polyatomic reactions. In the so-called sudden vector projection (SVP) model, the ability of a reactant mode in promoting the reaction depends on its coupling with the reaction coordinate at the transition state, which can be estimated in the sudden limit by the overlap of their corresponding normal mode vectors.<sup>116</sup> The SVP model, which emphasizes the importance of the transition state in controlling reactivity,<sup>117</sup> has been tested in many reactions, including some recent ones,<sup>55,118–127</sup> and its predictions have mostly been borne out.<sup>16,128,129</sup> The SVP model is not only able to predict mode specificity in reactions involving only a few atoms; it has been also validated in larger systems. For example, the Diels–Alder reaction between 2,3-dibromo-1,3-butadiene and maleic anhydride was found to be enhanced by exciting reactant rotational DOFs, in line with the prediction of SVP.<sup>130</sup> Similarly, SVP predictions<sup>131</sup> for the classic 1,3-dipolar cycloaddition reaction were also confirmed by recent QCT calculations on a full-dimensional PES.<sup>132</sup> In Figure 1, the mode specificity predicted by the SVP model in both the  $\text{Cl} + \text{CH}_3\text{OH} \rightarrow \text{HCl} + \text{CH}_3\text{O}/\text{CH}_2\text{OH}$  channels is shown to be consistent with the QCT results on an accurate PES.<sup>55</sup>

Interestingly, the sudden approximation, namely, the instantaneous nature of collisions relative to energy flow among different modes in the reactant, also leads to an approximate way to compute the state-to-state reaction probabilities. This model based on the TSWP approach of Welsch and Manthe<sup>76,77</sup> envisages a full collision process as two half-collision steps, each treated with Franck–Condon overlaps.<sup>133</sup> The results have been quite promising for direct reactions and could offer a computationally inexpensive way to quantify reaction dynamics.

There has recently been much interest in mode specificity in  $\text{X}^- + \text{YCH}_3$  type reactions.<sup>121,122,134</sup> Taking the example of the  $\text{F}^- + \text{CH}_3\text{I}$  case, the bimolecular nucleophilic substitution ( $\text{S}_{\text{N}}2$ ) channel features a submerged collinear Walden inversion saddle point leading to  $\text{FCH}_3 + \text{I}^-$ , flanked by pre- and post-transition state wells, while the proton transfer (PT) channel possesses several different saddle points leading to  $\text{HF} + \text{CH}_2\text{I}^-$ . Experimental investigations by Wester and co-workers found that the excitation of the CH stretching mode has a negligible effect on the  $\text{S}_{\text{N}}2$  channel while it promotes the PT channel.<sup>121</sup> These observations are consistent with the SVP model and confirmed by QCT calculations on an *ab initio*-based PES. Further QCT studies by Czako and co-workers have found moderate mode specificity in the  $\text{S}_{\text{N}}2$  involving other modes in the  $\text{CH}_3\text{I}$  reactant,<sup>49</sup> which is remarkable for this barrierless complex-forming reaction. This can be readily understood as the  $\text{S}_{\text{N}}2$  transition state depicts a collinear approach of the nucleophile from the back side of  $\text{CH}_3\text{I}$ , leading to the Walden inversion. On the other hand, the PT transition state involves the breaking of one C–H bond. To date, there is only one reliable QD study because of the large phase space involved.<sup>134</sup> Future work along this line is needed to further elucidate this issue.

On the basis of *ab initio* parametrized PESs,<sup>135–137</sup> the product state distributions of the  $\text{X}$  ( $\text{X} = \text{H}, \text{F}, \text{Cl}, \text{OH}$ ) +  $\text{C}_2\text{H}_6$  reactions have recently been investigated by Espinosa-Garcia, Corchado, and co-workers.<sup>138–141</sup> While generally in reasonably good agreement with experiment, there are still large quantitative differences. For the  $\text{Cl} + \text{C}_2\text{H}_6 \rightarrow \text{HCl} + \text{C}_2\text{H}_5$  reaction, for example, the calculated rotational distribution of the HCl product is hotter than experiment. More recently, Czako and co-workers reported a full-dimensional PIP PES for this reaction and obtained excellent agreement with experiment,

Quantum dynamic studies of reactive scattering are currently restricted to low-dimensional systems because of the so-called “dimensionality curse”, namely, the fact that the size of the problem ( $N$ ) increases exponentially with the number of DOFs.

underscoring the importance of global accuracy of the PES.<sup>54</sup> We note in passing that the SVP model can be used to predict product energy disposal, which is related to mode specificity of the reverse reaction. Such predictions are usually accurate for direct reactions.<sup>16,129</sup>

Despite its success, the SVP model can fail if its assumptions are not fulfilled. For example, if the reaction proceeds via a complex-forming mechanism that renders the sudden approximation invalid, the SVP predictions are known to be unreliable. It can also fail for other reasons. In a recent theoretical investigation, Liu et al. found that vibrational excitation of the OH reactant in its reaction with  $\text{HO}_2$  has a significant enhancement effect at low collision energies,<sup>127</sup> as shown in Figure 2a. This observation is at odds with the SVP prediction as this OH mode is a spectator. Detailed analysis revealed that the enhancement stems from a stronger interaction between the reactants due to the enlarged dipole of the vibrationally excited

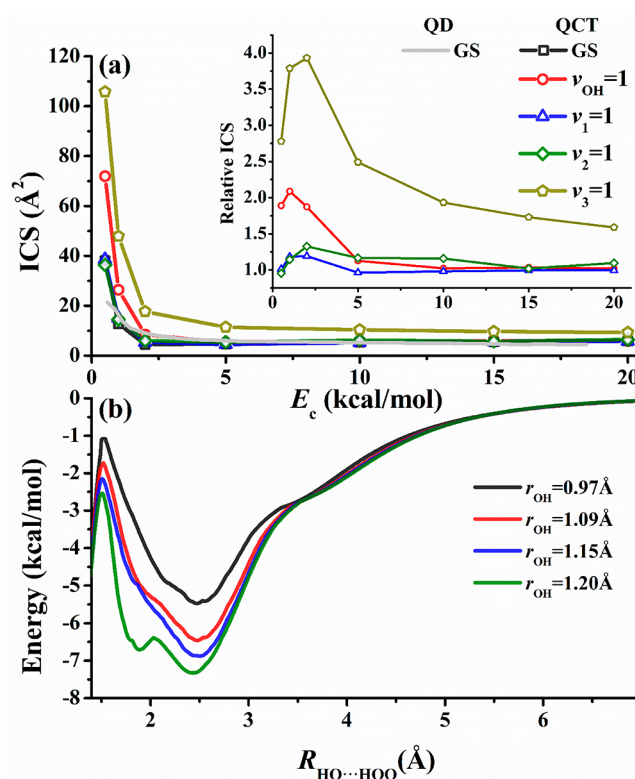


**Figure 2.** (a) Calculated excitation functions for  $\text{OH}(v_{\text{OH}}) + \text{HO}_2(v_1, v_2, v_3) \rightarrow \text{H}_2\text{O} + \text{O}_2$  with relative cross sections shown in the inset. (b) Interaction between OH (at different bond distances) and  $\text{HO}_2$  (fixed at its equilibrium) along the  $R_{\text{OH}\cdots\text{HOO}}$  distance at  $\text{HO}\cdots\text{HOO}$  well. Reproduced from ref 127 with permission. Copyright 2020 American Chemical Society.

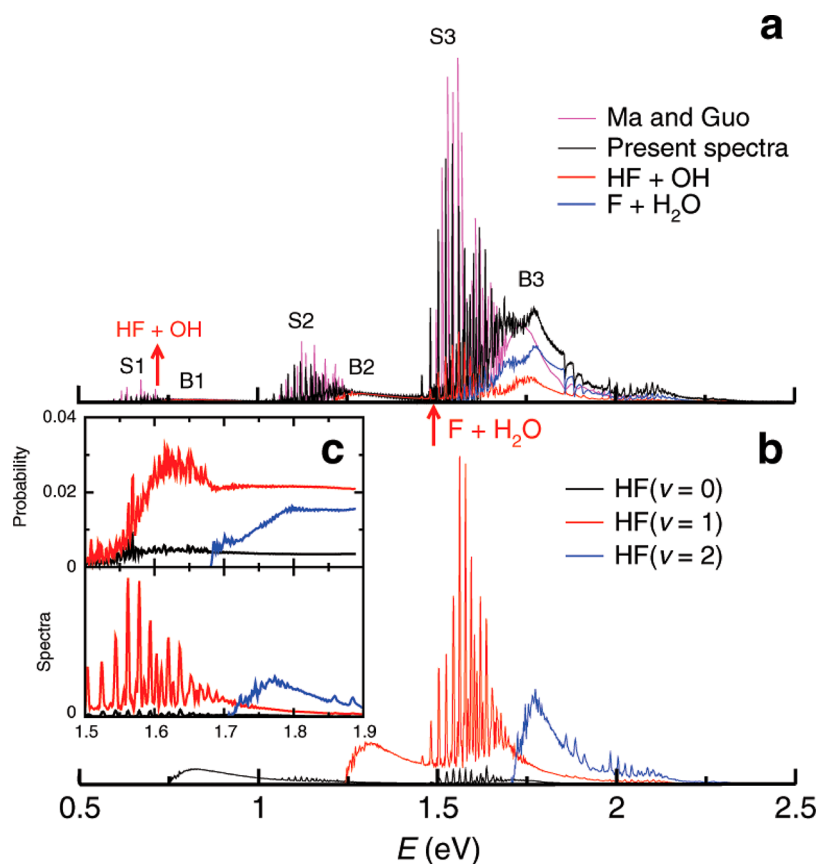


**Figure 3.** (a) Comparison of calculated photoelectron spectra the  $\text{FH}_2\text{O}^-$  anion with the earlier work (Ma and Guo<sup>151</sup>). The shape peaks stem from Feshbach resonances in the product well. (b) The HF vibrational state-resolved reactive flux spectra to HF + OH. (c) The comparison between the HF vibrational state-resolved reaction probabilities of the neutral reaction and the reactive flux spectra at the energy of 1.5–1.9 eV. Reproduced from ref 154 with permission. Copyright 2020.

OH reactant, as illustrated in Figure 2b. This is possible because there is a substantial potential well before the submerged transition state for this reaction, underscoring the complexity of reaction dynamics.

Dynamic resonances, which are metastable states embedded in the continuum, are now known to play an important role in many chemical reactions. Resonances are intrinsically a quantum effect and have two major types. A Feshbach resonance is related to a state in which energy is trapped in an internal mode and its coupling with the dissociation coordinate is weak, while a shape resonance is formed because of a potential well. Because resonance wave functions differ significantly from direct scattering ones, they often have unexpected influence on reactivity, because they extend time for the system to linger near the transition state. Their presence can be detected from DCSs and energy dependence of ICSs,<sup>13,14</sup> or alternatively by photodetachment of stable anions with geometries that resemble transition states in the neutral reactions.<sup>142,143</sup> Although their existence has been speculated for some time,<sup>144</sup> unequivocal experimental identifications have started to emerge only in recent years.<sup>14</sup> For example, the F + *para*-H<sub>2</sub> → HF + H reaction was found to be strongly influenced by Feshbach resonances supported by a post-transition state well, which significantly enhances the low-energy reactivity due to quantum tunneling.<sup>145</sup> Theory played a decisive role in assigning these resonances based on the clear nodal structures of the resonance wave functions. Of course, dynamical resonances are not restricted to the Feshbach type in the product channel.

Evidence of shape resonances has been reported for the F + H<sub>2</sub> reaction.<sup>146</sup> Very short-lived resonances have also been identified in the reaction of Cl with vibrationally excited HD, which have both Feshbach and shape characters.<sup>147</sup>

While dynamic resonances are well understood in triatomic systems,<sup>14</sup> as discussed above, their roles in reactive systems with four or more atoms are only beginning to be elucidated. With more DOFs, resonances show richer features but can be understood with the same principles. For example, both the F + H<sub>2</sub>O → HF + OH and F + CH<sub>3</sub>OH → HF + CH<sub>3</sub>O reactions feature a low reaction barrier and both pre- and post-transition state wells. Like the F + H<sub>2</sub> reaction discussed above, well-defined resonances have been found in the product wells by photodetachment experiments<sup>47,148–150</sup> supported by quantum scattering calculations.<sup>47,151,152</sup> These resonances are all associated with a vibrationally excited HF product and thus are Feshbach in nature. The calculated state-to-state reaction probabilities of the F + H<sub>2</sub>O reaction have a rich oscillatory structure, which have been attributed to resonances in both the pre- and post-transition state wells.<sup>153,154</sup> Recent quantum scattering calculations demonstrated unequivocally that the post-transition state resonances have a strong influence on reactivity,<sup>154</sup> as shown in Figure 3.

Similar to the F + H<sub>2</sub>O case, the F + CH<sub>4</sub> reaction has both pre- and postreaction wells. In a recent 8D WP study, prominent resonance structure is observed at low collision energies of the F + CHD<sub>3</sub> reaction.<sup>119</sup> It was argued that the pretransition state well of the reaction gives rise to long-lived resonances,<sup>155,156</sup>

which result in a stereodynamic force that affects the reaction dynamics. This reaction is a serious challenge to theory in both the accuracy of the PES and the high dimensionality of the dynamics. Recently, full dimensional DPEM including vibronic and spin-orbit couplings for this reaction have been reported,<sup>157</sup> and a 7D WP calculation beyond the BO approximation showed distinct nonadiabatic effects on the resonance features.<sup>158</sup>

Clearly, a resonance depends sensitively on the PES. As a result, comparison with measured resonance positions and widths provide a stringent assessment of the quality of the *ab initio* calculations and the resulting PES. This was illustrated in a recent study of the  $F + HD \rightarrow HF + D$  reaction, in which a more accurate PES was needed to reproduce experimentally observed resonance peaks.<sup>159</sup> The  $F + H_2O/CH_4/CH_3OH$  PESs have 6,<sup>160–162</sup> 12,<sup>163–165</sup> and 15 internal DOFs,<sup>47</sup> respectively, and the agreement with experiment resonance positions is a testament to the high accuracy of these high-dimensional PESs. These PESs are expected to provide reliable platforms for future dynamical studies.

We emphasize in passing that peaks in ICSs are not always associated with resonances. In a recent study of a heavy-light-heavy (HLH) reaction, namely  $Cl + CH_4 \rightarrow HCl + CH_3$ , such a peak has been shown to stem from reactivity oscillation of the HLH system, which has a classical origin, rather than being a quantum resonance.<sup>95</sup> Again, theory is instrumental in ruling out the resonance by calculating the delay time of scattering and by inspecting the scattering wave function. This work also represents a significant advance in quantum scattering theory in that calculating DCSs of a six-atom reaction is now possible, albeit in reduced dimensionality.

Roaming denotes a high-energy dynamical phenomenon that involves frustrated dissociation.<sup>166,167</sup> In the case of the prototypical  $H_2CO$  photodissociation near the  $H + HCO$  radical dissociation limit, for example, the roaming H atom can undergo large-amplitude orientational motion before abstracting H from HCO to form the  $H_2 + CO$  products, leading to product internal state distributions that differ dramatically from dissociation through the minimum-energy path and a tight transition state from  $H_2CO$  to the same products.<sup>168</sup> This example illustrates the importance of dynamics over the conventional transition-state theory defined by energy barriers. Statistically, the prevalence of roaming in the van der Waals region can be understood in terms of an entropic effect, which trumps energetics.<sup>169</sup> While roaming has been observed in many unimolecular reactions,<sup>169</sup> evidence of its involvement in bimolecular reactions has just started to emerge.<sup>53,170–176</sup> In a recent study, for example, Fu et al. reported roaming in the  $H + C_2H_4 \rightarrow H_2 + C_2H_3$  reaction. Using a QCT method on an *ab initio*-based global PES, these authors found two roaming pathways leading to distinctly different product distributions.<sup>53</sup> This and other examples suggest that roaming could be quite ubiquitous in bimolecular reactions involving radicals because of the flat potentials in the van der Waals regions. Similar large-amplitude dynamics have also been noted in ion-molecule reactions because of their long-range interactions.<sup>177,178</sup>

Most of the existing studies of roaming have been based on QCT.<sup>179</sup> While such studies have captured most dynamics features, there are serious issues concerning the influence of quantum effects in the dynamics. For instance, ZPE violation in the  $H + HCO$  channel of the  $H_2CO$  dissociation could conceivably affect the roaming dynamics.<sup>169</sup> To date, however, quantum treatments of roaming dynamics have been rare,<sup>173</sup>

apparently because of the large density of states involved in such high-energy collisions. This challenge is not easily met by reduced-dimensional quantum models as few DOFs are spectators at such high energies. Novel semiclassical methods that include quantum effects might be able to help.

As the size of the reaction system increases, the dynamics become more complicated because of the involvement of multiple nonequivalent product channels. In  $X^- + CH_3Y$  ( $X, Y = F, Cl, Br, I, OH$ , etc.) reactions, for example, the competition of the  $S_N2$  ( $CH_3X + Y^-$ ) and the PT ( $HX + CH_2Y^-$ ) channels has been a recent topic of dynamic investigations.<sup>49,121,122,180</sup> Similarly, product branching in neutral reactions has also attracted much current attention.<sup>51,55,165,181–184</sup> These dynamical studies were mostly made possible by global multichannel PESs.

The branching ratio for different product channels depends on energetic factors, such as the corresponding exoergicity and barrier height for each product channel. However, many other dynamical factors can be important. Hydrogen abstraction reactions from the two reactive centers of  $CH_3OH, X + CH_3OH \rightarrow HX + CH_3O/CH_2OH$  ( $X = H/F/Cl/OH$ ), exemplify such dynamics. For the  $Cl + CH_3OH \rightarrow HCl + CH_3O/CH_2OH$  reaction, the yield of the  $HCl + CH_3O$  product channel is negligible at low temperatures because its barrier is  $\sim 10$  kcal/mol, while the other channel is barrierless. At room temperature, the calculated branching ratio of the  $CH_3O$  channel is merely 0.02,<sup>55</sup> consistent with experiment. For the  $F + CH_3OH$  reaction, on the other hand, both channels are barrierless and exoergic. The calculated value for the  $CH_3O$  branching fraction is 0.40–0.43 within 200–1000 K, in reasonable agreement with available experimental measurements.<sup>182</sup> A statistical prediction would be that the  $HF + CH_3O$  channel should have only a branching fraction of 0.25, but this is apparently not the case. Detailed analysis of QCT results on a global PES attributed the nonstatistical branching ratio to the unique stereodynamics in the entrance channel for the abstraction from the OH moiety.<sup>183</sup>

At room temperature, the reaction cross section is summed over contributions from many partial waves, which classically correspond to different impact parameters. By lowering the collision energy, it is possible to reach a regime where one or few partial waves contribute. Furthermore, scattering at low and ultralow collision energies is strongly influenced by quantum effects, such as tunneling and resonances.<sup>11</sup> This pure quantum regime presents both challenges and opportunities to understand chemistry from a unique perspective.<sup>185,186</sup> Experimentally, cold collisions around 1 K have been realized in molecular beams either by slowing molecules using brute force<sup>5,9</sup> or by reducing the relative collisional velocity with small collision angles.<sup>10</sup> To date, however, there have been relatively few cross-beam studies on reactive scattering at low temperatures.<sup>187</sup> This is because such reactions, which typically involve radicals or ions, have necessarily no or small barriers. In both cases, it is difficult to create cold collision conditions in molecular beams with sufficiently large number densities. Theoretically, it is also challenging because the numerically more efficient WP approach requires long time propagation because of the low translational energy and large grids to accommodate long de Broglie wavelengths. TIQM methods are ideal, but they suffer from steep scaling with respect to the dimensionality of the problem.

The reaction  $F + H_2 \rightarrow HF + H$  serves as a good example for cold (1–10 K) chemistry. Despite a small barrier ( $\sim 1.8$  kcal/mol or 900 K) in the entrance channel, this reaction is known to

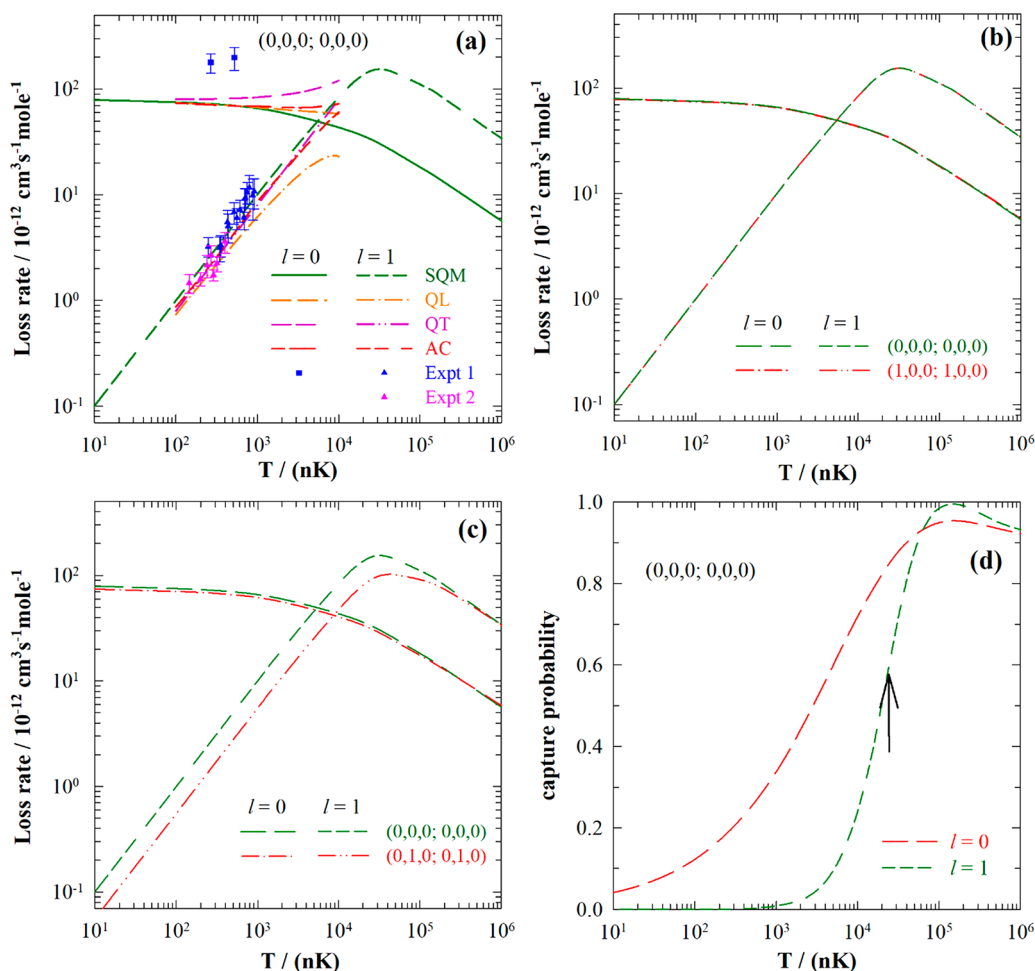


**Figure 4.** SQM results for the ultracold KRb + KRb reaction. (a) Comparison with experimental (Expt 1<sup>198</sup> and Expt 2<sup>237</sup>) and previous theoretical loss rates<sup>205</sup> for distinguishable and indistinguishable reactants. (b) Comparison of the loss rates for  $v_1 = v_2 = 0$  and 1 KRb reactants. (c) Comparison of the loss rates for  $j_1 = j_2 = 0$  and 1 KRb reactants. (d) Capture probabilities for the s and p waves. Reproduced from ref 203 with permission. Copyright 2020.

have significant reactivity at temperatures as low as 10 K.<sup>188</sup> To understand this surprising phenomenon, this reaction was recently studied at very low collision energies with crossed beams at a small angle, which revealed the reactivity is apparently due to a resonance.<sup>145</sup> WP and TIQM calculations on an accurate PES revealed that the tunneling resonance is of a Feshbach character formed in the product channel associated with a HF vibrational quantum number. Hence, the formation of HF in cold interstellar media is now recognized as a consequence of quantum effects. More recently, quantum scattering calculations have been extended to ultralow temperatures (up to 0.5 mK).<sup>189</sup> These quantum scattering calculations were performed with a TIQM method,<sup>190</sup> which is limited to atom–diatom reactive scattering with a relatively small number of channels. To improve scaling, it is desirable to use a WP-based method. Recently, some progress has been made by propagating the wave packet on different grids for different regions of the reaction path,<sup>78,81</sup> such that the relatively flat long-range interaction potential allows large grid spacing even when a very large range is needed to support the long de Broglie wave. Further work is highly desirable to formulate efficient algorithms for dealing with cold reactive collisions.

Chemical reactions have also been discovered in the ultracold ( $<1 \mu\text{K}$ ) regime. Ultracold KRb molecules, for example, have been created in single quantum states through a coherent two-

photon scheme from ultracold K and Rb atoms.<sup>191</sup> Collisions between these ultracold KRb molecules and K atoms are thought to contribute the loss of KRb in the trap. To understand the reaction dynamics, a TIQM method was applied to investigate this barrierless complex-forming reaction.<sup>192</sup> Although only a single partial wave dominates, such state-to-state quantum scattering calculations are still extremely challenging because of the large number of states in the  $\text{K}_2\text{Rb}$  well. However, the chaotic nature of the wave functions in the well also suggests an alternative treatment of the dynamics, in which the reactivity is controlled by the capture of the reactants by the  $\text{K}_2\text{Rb}$  complex. This statistical quantum mechanical (SQM) method<sup>193,194</sup> should offer an efficient way to determine reactivity at ultracold conditions accurately. Indeed, SQM has been shown to give a reasonably good approximation of the exact TIQM results for the  $\text{Li} + \text{LiYb}$  reaction in the ultracold regime.<sup>195</sup> In some other cases, however, it was shown that the reactivity may not be entirely determined by the long-range interaction and that features in the strongly interacting region can sometimes be important, even at low temperatures.<sup>196,197</sup>

Ultracold reaction between two KRb molecules in single quantum states has also been reported to produce  $\text{K}_2 + \text{Rb}_2$  through a long-lived  $\text{K}_2\text{Rb}_2$  complex.<sup>198,199</sup> The loss rate of KRb molecules in the trap was shown to be controlled by quantum statistics.<sup>198</sup> The reaction rate between indistinguishable



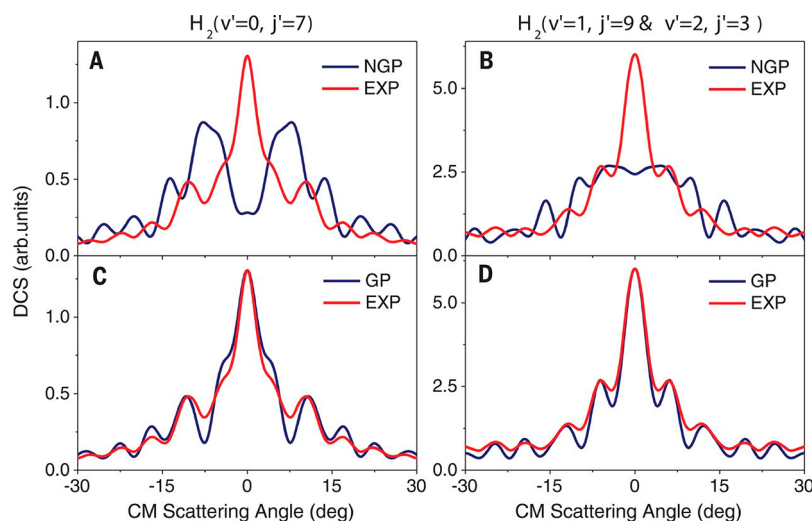


**Figure 5.** Differential cross sections (DCSs) for the  $\text{H} + \text{HD} \rightarrow \text{H}_2 + \text{D}$  reaction obtained with (GP) and without the geometric phase (NGP) and comparison with experimentally measured angular distribution (EXP). Reproduced from ref 217 with permission. Copyright 2018.

Fermionic KRb increases linearly with temperature, following the Wigner threshold law. This is due to the fact that the antisymmetry of the Fermionic wave function requires the lowest partial wave to be the  $p$ -wave ( $l = 1$ ). The reaction thus occurs via tunneling through the centrifugal barrier, which is remarkable given the heavy mass of the reactants. The tunneling stems from the long de Broglie wavelength at the ultracold temperature. On the other hand, the loss rate between distinguishable KRb has no temperature dependence, because the reaction is dominated by the  $s$ -wave ( $l = 0$ ). Given the large number of states supported by the deep  $\text{K}_2\text{Rb}_2$  well and the tiny exoergicity ( $\sim 10 \text{ cm}^{-1}$ ),<sup>200</sup> it is impossible to carry out state-to-state quantum scattering calculations with the existing algorithm and computer power. As suggested in the KRb + K system mentioned above, however, the high density of states and long lifetime<sup>200,201</sup> in such systems<sup>198,199</sup> allow an SQM treatment. Very recently, SQM methods have been developed to investigate diatom–diatom capture dynamics.<sup>202,203</sup> The application of a full-dimensional SQM method to the KRb + KRb reaction showed excellent reproduction of the experimental observations (Figure 4a), describing accurately the tunneling through the centrifugal barrier in the  $p$ -wave capture (Figure 4d).<sup>203</sup> This method is also able to predict loss rates for internally excited reactants (Figure 4b,c), as well as product state distributions.<sup>204</sup> Advances in treating the dynamics dominated by quantum effects are needed to gain further insight into the emerging field of cold chemistry.

An important characteristic of cold collision is that the kinetic energy is so small that the details of the intermolecular interaction at the extremely long-range becomes important. This demands an ultra-accurate description of the long-range potentials. Conventional procedures of fitting *ab initio* points are insufficient because they do not guarantee the correct asymptotic behavior. As a result, a physically inspired functional form for dispersion and electrostatic interactions is often more appropriate and they can be parametrized by high-level *ab initio* calculations.<sup>205,206</sup> A more accurate representation of the long-range PES, using machine learning approaches such as kernel-based regression with correct long-range behaviors,<sup>207</sup> could offer a promising alternative. A related challenge is to describe the influence of external fields on ultracold collisions, which are capable of overcoming weak long-range intermolecular inter-

actions. Therefore, some of the conservation laws in zero field are no longer valid, which requires different treatments of the quantum scattering.<sup>208</sup> Strong interaction with experimentalists is highly desirable in this field.

Although most reactions occur on the ground electronic state, the breakdown of the adiabatic BO approximation has been seen in an increasing number of systems. A commonly encountered electronic degeneracy is CIs, which form an  $N-2$ -dimensional crossing seam for a system with  $N$  internal DOFs.<sup>65,66</sup> A definitive understanding of the reaction dynamics thus needs to go beyond the adiabatic approximation, which is challenging. This is typically done within the diabatic representation,<sup>209</sup> which avoids cusps in the adiabatic PES and singularity in derivative coupling, namely, the change of electronic properties with respect to nuclear motion, at the CI seam. The diabatic representation poses no fundamental difficulties for dynamics as the scalar adiabatic PES is replaced by DPEM. As discussed, there has been important progress in constructing analytic global DPEMs from high-level *ab initio* data.

An important issue in nonadiabatic reactive scattering is the effect of the geometric phase (GP), which arises in the adiabatic representation where the electronic wave function in a path encircling the CI acquires a phase. This phase is geometric because it does not depend on the exact path but on whether or not the path encircles the CI. It causes the electronic wave function to be double-valued around the CI, which has to be compensated by a double-valued nuclear wave function to maintain single-valuedness of the total wave function.<sup>210,211</sup> It is important to note that GP is absent in the diabatic representation, as the double-valuedness in the adiabatic representation is removed by diabatization. However, the use of the diabatic representation loses the appeal and clarity of the BO PES, as it necessarily requires more than one state. GP can have a dramatic impact on dynamics in the adiabatic representation.<sup>67,212,213</sup> A good example is the  $\text{H} + \text{H}_2$  reaction, for which the ground-state PES forms a CI with an upper state in  $D_{3h}$  geometry at  $\sim 2.75 \text{ eV}$  above the reactant asymptote.<sup>214</sup> As a result, two different reaction paths between the same reactant and product arrangement channels form a circle around the CI and could interfere because of GP.<sup>215,216</sup> The search for the GP in this reaction has led to a recent experiment in which the interference pattern was observed in the product DCS of the  $\text{H} +$

HD  $\rightarrow$  H<sub>2</sub> + D reaction above the energy of the CI.<sup>217</sup> As shown in Figure 5, this interference pattern is in agreement with WP dynamics in a diabatic representation but differs from that obtained on the ground-state adiabatic PES without the GP included. Here, the WP approach is necessary because of the high energy in the experiment. More recently, oscillations with respect to the collision energy have been detected, reinforcing the existence of two topologically different reaction paths around the CI, according to detailed topological analysis.<sup>218</sup> One such reaction path is the well-known direct one, while the other involves some roaming. The deeper understanding of the nonadiabatic dynamics in this simplest reaction is not possible without detailed theoretical calculations.

Despite a long history in searching for the GP effect in the H + H<sub>2</sub> reaction, it has eluded detection until now, because of the average over many partial waves.<sup>212</sup> It follows that the GP effect might be more readily detected when only one or a few partial waves are present. Recent calculations using a hyperspherical coordinate TIQM method<sup>219</sup> have confirmed this speculation in both the H + H<sub>2</sub> and H + O<sub>2</sub> reactions at low and ultralow collision energies.<sup>220,221</sup> These intriguing theoretical results challenge experimentalists to verify the predictions.

Nonadiabatic effects are also found to play an important role in other reactions. An extensively studied class of reactions involves hydrogen abstraction by halogen atoms.<sup>75,157,222,223</sup> Because of the *p*-hole in these atoms, three coupled electronic states are involved in the reactant channel, and asymptotically they correspond to the <sup>2</sup>P states of the halogen atoms. With relativistic spin-orbit coupling, they are split into the ground (<sup>2</sup>P<sub>3/2</sub>) and excited (<sup>2</sup>P<sub>1/2</sub>) spin-orbit states. The approach of the reactant to the halogen atoms lifts the degeneracy, and only one of the three doublet states is reactive. There is a CI in the entrance channel that affects the reaction dynamics.<sup>155</sup> Nonadiabatic transitions in the F + CHD<sub>3</sub>  $\rightarrow$  HF + CD<sub>3</sub> reaction on an *ab initio* DPEM<sup>157</sup> are found to increase the reactivity compared to BO theory and are more prominent than in triatomic reactions previously studied (Figure 6).<sup>158,224</sup>

A future challenge in understanding the nonadiabatic effect is the characterization of dynamics of a four-atom reaction. A prototype is the OH(A) + H<sub>2</sub> process, which can lead to reactive quenching (H<sub>2</sub>O + H) or nonreactive quenching (OH(X) + H<sub>2</sub>),<sup>225,226</sup> through CIs between the ground and excited state PESs.<sup>227,228</sup> Attempts to map out the corresponding full-dimensional DPEM have only recently become successful<sup>229–231</sup> because of the existence of several diabatic states, complex CI seams, and high permutation symmetry. Dynamical calculations are also difficult because of the approximately 4 eV of energy release. So far, only reduced-dimensional quantum and trajectory surface hopping calculations have been reported,<sup>229,232</sup> but there exist multiple nonadiabatic pathways in this prototypical system involving breaking of different bonds.<sup>233</sup> Hence, a complete understanding will have to wait for a full-dimensional nonadiabatic quantum scattering calculation. Interestingly, QCT calculations initiated at the CI seam on the adiabatic PES of the ground state found the reactive quenching is preferred,<sup>234,235</sup> in agreement with experimental reports.<sup>225,226</sup> However, a surface hopping study by Collins et al. on a 3-state DPEM indicated that the nonreactive quenching dominates over the reactive quenching,<sup>229</sup> in stark contrast to experimental observations. This apparent disagreement is expected to stimulate more future investigations.

In this Perspective, we survey the recent advances in scattering theory for bimolecular reactions in the gas phase since 2016 and

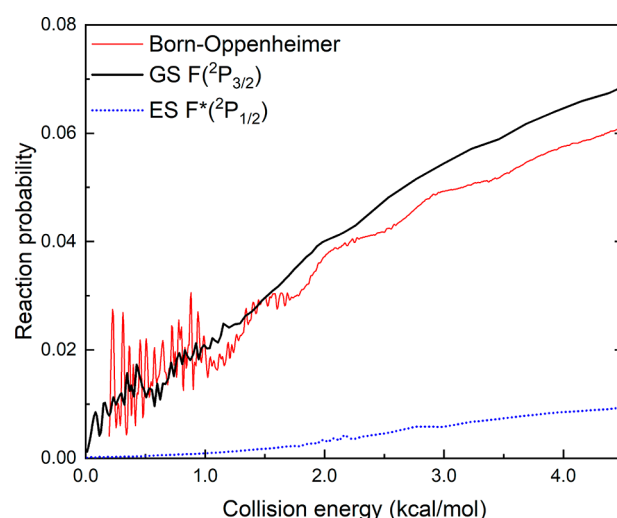


**Figure 6.** F + CHD<sub>3</sub>  $\rightarrow$  HF + CD<sub>3</sub> reaction probabilities: results of nonadiabatic calculations for F(<sup>2</sup>P<sub>3/2</sub>) + CHD<sub>3</sub> and F\*(<sup>2</sup>P<sub>1/2</sub>) + CHD<sub>3</sub> are displayed by black solid line (GS = ground state) and dotted blue line (ES = excited state), respectively, and compared to results for F(<sup>2</sup>P<sub>3/2</sub>) + CHD<sub>3</sub> obtained within the Born–Oppenheimer approximation (thin red line). Reproduced from ref 158 with permission. Copyright 2020.

identify some exciting new challenges in this field. One significant recent advance is our ability to map out global high-dimensional PESs and DPEMs for reactive systems from high-level *ab initio* calculations with high fidelity, often assisted by machine learning algorithms. This has enabled accurate calculations of dynamical attributes that can be directly compared with experiment, leading to better understanding of reaction dynamics. It is probably reasonable to conclude that this long-standing bottleneck in reaction dynamics studies, namely, the construction of highly accurate PESs for reactive systems, is now largely removed. Future work in this direction will place an emphasis on large reactive systems and coupled multistate problems.<sup>236</sup>

It is probably reasonable to conclude that this long-standing bottleneck in reaction dynamics studies, namely, the construction of highly accurate PESs for reactive systems, is now largely removed. On the other hand, progress in scattering theory has been relatively slow.

On the other hand, progress in scattering theory has been relatively slow. Apart from small (3–4 atoms) systems, most dynamical investigations have been performed using QCT methods. Although inexpensive and insightful, the accuracy of these methods is not guaranteed because of the intrinsic quantum nature of molecular systems. Despite recent reports of higher-dimensional quantum reactive scattering studies, the exponential scaling of both memory and CPU costs with respect to the dimensionality limits future development. This “dimensionality curse” might be dispelled only with quantum computers in the future. However, more pragmatic approaches,

preferably with classical trajectories, might be possible. The recent attempts using ring-polymer molecular dynamics exemplified such a strategy.

We expect continuing interest to understand dynamics in prototypical reactions involving only a few atoms. These systems provide an ideal proving ground to explore key issues, such as mode specificity, nonadiabaticity, resonances, tunneling, and steric effects. New dynamical calculations on high-accuracy potential energy surfaces will continue to shed light on experimental observations made with increasingly more sophisticated instruments and in some cases challenge experiment. Future studies might focus more on explorations of reaction dynamics under nonthermal conditions, such as highly electronically or internally excited and aligned/oriented reactants, which offers a potent venue to discover novel reaction channels and to understand reactions under extreme conditions. We also anticipate expansion of theoretical studies of reactions that involve many atoms, which possess additional complexity. Energy flow in larger systems might start to compete with reactive channels, particularly when reaction intermediates are present along the reaction path.

## AUTHOR INFORMATION

### Corresponding Authors

**Jun Li** – School of Chemistry and Chemical Engineering & Chongqing Key Laboratory of Theoretical and Computational Chemistry, Chongqing University, Chongqing 401331, China; [orcid.org/0000-0003-2392-8322](https://orcid.org/0000-0003-2392-8322); Email: [jli15@cqu.edu.cn](mailto:jli15@cqu.edu.cn)

**Bin Zhao** – Theoretische Chemie, Fakultät für Chemie, Universität Bielefeld, D-33615 Bielefeld, Germany; [orcid.org/0000-0001-5862-7402](https://orcid.org/0000-0001-5862-7402); Email: [bin.zhao@uni-bielefeld.de](mailto:bin.zhao@uni-bielefeld.de)

**Daiqian Xie** – Institute of Theoretical and Computational Chemistry, School of Chemistry and Chemical Engineering, Nanjing University, Nanjing 210023, China; [orcid.org/0000-0001-7185-7085](https://orcid.org/0000-0001-7185-7085); Email: [dqxie@nju.edu.cn](mailto:dqxie@nju.edu.cn)

**Hua Guo** – Department of Chemistry and Chemical Biology, University of New Mexico, Albuquerque, New Mexico 87131, United States; [orcid.org/0000-0001-9901-053X](https://orcid.org/0000-0001-9901-053X); Email: [hguo@unm.edu](mailto:hguo@unm.edu)

Complete contact information is available at:

<https://pubs.acs.org/10.1021/acs.jpcllett.0c02501>

### Notes

The authors declare no competing financial interest.

### Biographies



**Jun Li** is Professor of Chemistry at Chongqing University, China. He received his Bachelor and Doctoral degrees from Sichuan University.

He worked with Prof. Sheng-Hsien Lin as a visiting student at National Chiao-Tung University on photochemistry for five months. After a three-year postdoctoral research with Prof. Hua Guo at University of New Mexico, he joined Chongqing University as an independent PI. With a Humboldt Fellowship for Experienced Researchers, he worked with Prof. Jörg Behler at Georg-August-Universität Göttingen, Germany. His research interests include potential energy surfaces, reaction kinetics, and dynamics for gas-phase systems.



**Bin Zhao** is currently a postdoctoral associate with Prof. Dr. Uwe Manthe at Universität Bielefeld, Germany. He received his B.S. degree from Dalian University of Technology (China) and his Ph.D. from Nanyang Technological University (Singapore). He did his first postdoc with Prof. Hua Guo at University of New Mexico before joining Prof. Manthe's group with a Humboldt research fellowship. His research interests focus on high-dimensional quantum reactive scattering at the state-to-state level.



**Daiqian Xie** is a Distinguished Professor at Nanjing University, China. He received his B.S. degree from Sichuan University in 1983 and Ph.D. degree in Physical Chemistry from Jilin University in 1988. After a postdoctoral appointment at Jilin University from 1988 to 1991, he became a professor at Sichuan University from 1991 to 2001. He was a visiting professor at University of New Mexico, Duke University, National University of Singapore, and Nanyang Technological University. His research focuses on the construction of reliable molecular potential energy surface and quantum state-resolved reaction dynamics.



**Hua Guo** is a Distinguished Professor at University of New Mexico specializing in theoretical and computational chemistry. He received his B.S and M.S. degrees in China, and his D.Phil. from Sussex University (U.K.) with the late Prof. John Murrell. He did a postdoc with Prof. George Schatz at Northwestern University before starting his independent career. He has published more than 500 peer-reviewed articles, and his research interests cover mechanisms, dynamics, and kinetics of gas-phase reactions, photochemistry, and surface reactions. He was elected Fellow of American Physical Society in 2013.

## ACKNOWLEDGMENTS

J.L. thanks the National Natural Science Foundation of China (Grant Nos. 21973009 and 21973109), Chongqing Municipal Natural Science Foundation (cstc2019jcyj-msxmX0087), and Alexander von Humboldt Foundation (Humboldt Fellowship for Experienced Researchers) for support. B.Z. thanks Prof. Dr. Uwe Manthe for support and acknowledges previous support from Alexander von Humboldt Foundation. D.X. thanks the National Natural Science Foundation of China (Grant Nos. 21733006 and 21590802) for support. H.G. acknowledges support from the Department of Energy (Grant No. DE-SC0015997), Army Research Office (Grant No. W911NF-19-1-0283), and Alexander von Humboldt Foundation for a Humboldt Research Award.

## REFERENCES

- (1) Levine, R. D. *Molecular Reaction Dynamics*; Cambridge University Press: Cambridge, 2005.
- (2) Lee, Y. T. Molecular beam studies of elementary chemical reactions. *Science* **1987**, *236*, 793–798.
- (3) Zare, R. N. Laser control of chemical reactions. *Science* **1998**, *279*, 1875–1879.
- (4) Yang, X. State-to-state dynamics of elementary bimolecular reactions. *Annu. Rev. Phys. Chem.* **2007**, *58*, 433–459.
- (5) van de Meerakker, S. Y. T.; Bethlem, H. L.; Vanhaecke, N.; Meijer, G. Manipulation and control of molecular beams. *Chem. Rev.* **2012**, *112*, 4828–4878.
- (6) Liu, K. Perspective: Vibrational-induced steric effects in bimolecular reactions. *J. Chem. Phys.* **2015**, *142*, 080901.
- (7) Pan, H.; Liu, K.; Caracciolo, A.; Casavecchia, P. Crossed beam polyatomic reaction dynamics: recent advances and new insights. *Chem. Soc. Rev.* **2017**, *46*, 7517–7547.
- (8) Meyer, J.; Wester, R. Ion–molecule reaction dynamics. *Annu. Rev. Phys. Chem.* **2017**, *68*, 333–353.
- (9) Narevicius, E.; Raizen, M. G. Toward cold chemistry with magnetically decelerated supersonic beams. *Chem. Rev.* **2012**, *112*, 4879–4889.
- (10) Jankunas, J.; Osterwalder, A. Cold and controlled molecular beams: Production and applications. *Annu. Rev. Phys. Chem.* **2015**, *66*, 241–262.
- (11) Bohn, J. L.; Rey, A. M.; Ye, J. Cold molecules: Progress in quantum engineering of chemistry and quantum matter. *Science* **2017**, *357*, 1002–1010.
- (12) Balucani, N.; Capozza, G.; Leonori, F.; Segoloni, E.; Casavecchia, P. Crossed molecular beam reactive scattering: from simple triatomic to multichannel polyatomic reactions. *Int. Rev. Phys. Chem.* **2006**, *25*, 109–163.
- (13) Liu, K. Quantum dynamical resonances in chemical reactions: From A + BC to polyatomic systems. *Adv. Chem. Phys.* **2012**, *149*, 1–46.
- (14) Wang, T.; Yang, T.; Xiao, C.; Sun, Z.; Zhang, D.; Yang, X.; Weichman, M. L.; Neumark, D. M. Dynamical resonances in chemical reactions. *Chem. Soc. Rev.* **2018**, *47*, 6744–6763.
- (15) Althorpe, S. C.; Clary, D. C. Quantum scattering calculations on chemical reactions. *Annu. Rev. Phys. Chem.* **2003**, *54*, 493–529.
- (16) Guo, H.; Jiang, B. The sudden vector projection model for reactivity: Mode specificity and bond selectivity made simple. *Acc. Chem. Res.* **2014**, *47*, 3679–3685.
- (17) Zhang, D. H.; Guo, H. Recent advances in quantum dynamics of bimolecular reactions. *Annu. Rev. Phys. Chem.* **2016**, *67*, 135–158.
- (18) Guo, H.; Yarkony, D. R. Accurate nonadiabatic dynamics. *Phys. Chem. Chem. Phys.* **2016**, *18*, 26335–26352.
- (19) Braams, B. J.; Bowman, J. M. Permutationally invariant potential energy surfaces in high dimensionality. *Int. Rev. Phys. Chem.* **2009**, *28*, 577–606.
- (20) Jiang, B.; Li, J.; Guo, H. Potential energy surfaces from high fidelity fitting of ab initio points: The permutation invariant polynomial-neural network approach. *Int. Rev. Phys. Chem.* **2016**, *35*, 479–506.
- (21) Qu, C.; Yu, Q.; Bowman, J. M. Permutationally invariant potential energy surfaces. *Annu. Rev. Phys. Chem.* **2018**, *69*, 151–175.
- (22) Fu, B.; Zhang, D. H. Ab initio potential energy surfaces and quantum dynamics for polyatomic bimolecular reactions. *J. Chem. Theory Comput.* **2018**, *14*, 2289–2303.
- (23) Dawes, R.; Quintas-Sánchez, E. The construction of ab initio based potential energy surfaces. *Rev. Comput. Chem.* **2018**, *31*, 199–263.
- (24) Krems, R. V. Bayesian machine learning for quantum molecular dynamics. *Phys. Chem. Chem. Phys.* **2019**, *21*, 13392–13410.
- (25) Welsch, R.; Manthe, U. Thermal flux based analysis of state-to-state reaction probabilities. *Mol. Phys.* **2012**, *110*, 703–715.
- (26) Czakó, G.; Bowman, J. M. Reaction dynamics of methane with F, O, Cl, and Br on ab initio potential energy surfaces. *J. Phys. Chem. A* **2014**, *118*, 2839–2864.
- (27) Li, J.; Jiang, B.; Song, H.; Ma, J.; Zhao, B.; Dawes, R.; Guo, H. From ab initio potential energy surfaces to state-resolved reactivities: The X + H<sub>2</sub>O ↔ HX + OH (X = F, Cl, and O(<sup>3</sup>P)) reactions. *J. Phys. Chem. A* **2015**, *119*, 4667–4687.
- (28) Szabó, I.; Czakó, G. Dynamics and novel mechanisms of S<sub>N</sub>2 reactions on ab initio analytical potential energy surfaces. *J. Phys. Chem. A* **2017**, *121*, 9005–9019.
- (29) Fu, B.; Shan, X.; Zhang, D. H.; Clary, D. C. Recent advances in quantum scattering calculations on polyatomic bimolecular reactions. *Chem. Soc. Rev.* **2017**, *46*, 7625–7649.
- (30) Zhao, B.; Guo, H. State-to-state quantum reactive scattering in four-atom systems. *WIREs: Comput. Mol. Sci.* **2017**, *7*, No. e1301.
- (31) Pratihari, S.; Ma, X.; Homayoon, Z.; Barnes, G. L.; Hase, W. L. Direct chemical dynamics simulations. *J. Am. Chem. Soc.* **2017**, *139*, 3570–3590.
- (32) Dawes, R.; Ndengué, S. A. Single- and multireference electronic structure calculations for constructing potential energy surfaces. *Int. Rev. Phys. Chem.* **2016**, *35*, 441–478.
- (33) Bartlett, R. J.; Musiał, M. Coupled-cluster theory in quantum chemistry. *Rev. Mod. Phys.* **2007**, *79*, 291–352.
- (34) Werner, H.-J. Matrix-formulated direct multiconfiguration self-consistent field and multiconfiguration reference configuration-interaction methods. *Adv. Chem. Phys.* **2007**, *69*, 1–62.
- (35) Shiozaki, T.; Werner, H.-J. Multireference explicitly correlated F12 theories. *Mol. Phys.* **2013**, *111*, 607–630.

- (36) Chen, J.; Su, N. Q.; Xu, X.; Zhang, D. H. Accurate potential energy surfaces for hydrogen abstraction reactions: A benchmark study on the XYG3 doubly hybrid density functional. *J. Comput. Chem.* **2017**, *38*, 2326–2334.
- (37) Györi, T.; Olasz, B.; Paragi, G.; Czako, G. Effects of the level of electronic structure theory on the dynamics of the  $F^- + CH_3I$  reaction. *J. Phys. Chem. A* **2018**, *122*, 3353–3364.
- (38) Tasi, D. A.; Györi, T.; Czako, G. On the development of a gold-standard potential energy surface for the  $OH^- + CH_3I$  reaction. *Phys. Chem. Chem. Phys.* **2020**, *22*, 3775–3778.
- (39) Liu, Y.; Bai, M.; Song, H.; Xie, D.; Li, J. Anomalous kinetics of the reaction between OH and  $HO_2$  on an accurate triplet state potential energy surface. *Phys. Chem. Chem. Phys.* **2019**, *21*, 12667–12675.
- (40) Czako, G.; Györi, T.; Olasz, B.; Papp, D.; Szabó, I.; Tajti, V.; Tasi, D. A. Benchmark ab initio and dynamical characterization of the stationary points of reactive atom + alkane and  $S_N2$  potential energy surfaces. *Phys. Chem. Chem. Phys.* **2020**, *22*, 4298–4312.
- (41) Werner, H.-J.; Knowles, P. J.; Manby, F. R.; Black, J. A.; Doll, K.; Heßelmann, A.; Kats, D.; Köhn, A.; Korona, T.; Kreplin, D. A.; et al. The Molpro quantum chemistry package. *J. Chem. Phys.* **2020**, *152*, 144107.
- (42) Cui, J.; Krems, R. V. Efficient non-parametric fitting of potential energy surfaces for polyatomic molecules with Gaussian processes. *J. Phys. B: At., Mol. Opt. Phys.* **2016**, *49*, 224001.
- (43) Behler, J. First principles neural network potentials for reactive simulations of large molecular and condensed systems. *Angew. Chem., Int. Ed.* **2017**, *56*, 12828–12840.
- (44) Bunker, P. R.; Jensen, P. *Molecular Symmetry and Spectroscopy*; NRC Research Press: Ottawa, 1998.
- (45) Bartók, A. P.; Kondor, R.; Csányi, G. On representing chemical environments. *Phys. Rev. B: Condens. Matter Mater. Phys.* **2013**, *87*, 184115.
- (46) Jiang, B.; Li, J.; Guo, H. High-fidelity potential energy surfaces for gas phase and gas-surface scattering processes from machine learning. *J. Phys. Chem. Lett.* **2020**, *11*, 5120–5131.
- (47) Weichman, M. L.; DeVine, J. A.; Babin, M. C.; Li, J.; Guo, L.; Ma, J.; Guo, H.; Neumark, D. M. Feshbach resonances in the exit channel of the  $F + CH_3OH \rightarrow HF + CH_3O$  reaction observed using transition-state spectroscopy. *Nat. Chem.* **2017**, *9*, 950–955.
- (48) Li, J.; Xie, C.; Guo, H. Kinetics and dynamics of the  $C(^3P) + H_2O$  reaction on a full-dimensional accurate triplet state potential energy surface. *Phys. Chem. Chem. Phys.* **2017**, *19*, 23280–23288.
- (49) Olasz, B.; Szabo, I.; Czako, G. High-level ab initio potential energy surface and dynamics of the  $F^- + CH_3I$   $S_N2$  and proton-transfer reactions. *Chem. Sci.* **2017**, *8*, 3164–3170.
- (50) Lu, X.; Shao, K.; Fu, B.; Wang, X.; Zhang, D. H. An accurate full-dimensional potential energy surface and quasiclassical trajectory dynamics of the  $H + H_2O_2$  two-channel reaction. *Phys. Chem. Chem. Phys.* **2018**, *20*, 23095–23105.
- (51) Zuo, J.; Chen, Q.; Hu, X.; Guo, H.; Xie, D. Dissection of the multichannel reaction of acetylene with atomic oxygen: from the global potential energy surface to rate coefficients and branching dynamics. *Phys. Chem. Chem. Phys.* **2019**, *21*, 1408–1416.
- (52) Yao, Q.; Xie, C.; Guo, H. Competition between proton transfer and proton isomerization in the  $N_2 + HOC^+$  reaction on an ab initio-based global potential energy surface. *J. Phys. Chem. A* **2019**, *123*, 5347–5355.
- (53) Fu, Y.-L.; Lu, X.; Han, Y.-C.; Fu, B.; Zhang, D. H.; Bowman, J. M. Collision-induced and complex-mediated roaming dynamics in the  $H + C_2H_4 \rightarrow H_2 + C_2H_3$  reaction. *Chem. Sci.* **2020**, *11*, 2148–2154.
- (54) Papp, D.; Tajti, V.; Györi, T.; Czako, G. Theory finally agrees with experiment for the dynamics of the  $Cl + C_2H_6$  reaction. *J. Phys. Chem. Lett.* **2020**, *11*, 4762–4767.
- (55) Lu, D.; Li, J.; Guo, H. Comprehensive dynamical investigations on the  $Cl + CH_3OH \rightarrow HCl + CH_3O/CH_2OH$  reaction: Validation of experiment and dynamical insights. *CCS Chem.* **2020**, *2*, 882–894.
- (56) Lu, D.; Behler, J.; Li, J. Accurate global potential energy surfaces for the  $H + CH_3OH$  reaction by neural network fitting with permutation invariance. *J. Phys. Chem. A* **2020**, *124*, 5737–5745.
- (57) Zuo, J.; Chen, Q.; Hu, X.; Guo, H.; Xie, D. Theoretical investigations of rate coefficients for  $H + O_3$  and  $HO_2 + O$  reactions on a full-dimensional potential energy surface. *J. Phys. Chem. A* **2020**, *124*, 6427–6437.
- (58) Li, J.; Varga, Z.; Truhlar, D. G.; Guo, H. Many-body permutationally invariant polynomial neural network potential energy surface for  $N_4$ . *J. Chem. Theory Comput.* **2020**, *16*, 4822–4832.
- (59) Qu, C.; Bowman, J. M. A fragmented, permutationally invariant polynomial approach for potential energy surfaces of large molecules: Application to N-methyl acetamide. *J. Chem. Phys.* **2019**, *150*, 141101.
- (60) Chen, R.; Shao, K.; Fu, B.; Zhang, D. H. Fitting potential energy surfaces with fundamental invariant neural network. II. Generating fundamental invariants for molecular systems with up to ten atoms. *J. Chem. Phys.* **2020**, *152*, 204307.
- (61) Yang, K. R.; Xu, X.; Truhlar, D. G. Anchor points reactive potential for bond-breaking reactions. *J. Chem. Theory Comput.* **2014**, *10*, 924–933.
- (62) Smith, J. S.; Isayev, O.; Roitberg, A. E. ANI-1: an extensible neural network potential with DFT accuracy at force field computational cost. *Chem. Sci.* **2017**, *8*, 3192–3203.
- (63) Unke, O. T.; Meuwly, M. PhysNet: A neural network for predicting energies, forces, dipole moments, and partial charges. *J. Chem. Theory Comput.* **2019**, *15*, 3678–3693.
- (64) Vargas-Hernández, R. A.; Guan, Y.; Zhang, D. H.; Krems, R. V. Bayesian optimization for the inverse scattering problem in quantum reaction dynamics. *New J. Phys.* **2019**, *21*, 022001.
- (65) Yarkony, D. R. Diabatical conical intersections. *Rev. Mod. Phys.* **1996**, *68*, 985–1013.
- (66) Domcke, W.; Yarkony, D. R.; Köppel, H. *Conical Intersections: Electronic Structure, Dynamics and Spectroscopy*; World Scientific: Singapore, 2004.
- (67) Yarkony, D. R. Nonadiabatic quantum chemistry - past, present and future. *Chem. Rev.* **2012**, *112*, 481–498.
- (68) Mead, C. A.; Truhlar, D. G. Conditions for the definition of a strictly diabatic electronic basis for molecular systems. *J. Chem. Phys.* **1982**, *77*, 6090–6098.
- (69) Baer, M. Adiabatic and diabatic representations for atom-diatom collisions: Treatment of the three-dimensional case. *Chem. Phys.* **1976**, *15*, 49–57.
- (70) Evenhuis, C. R.; Collins, M. A. Interpolation of diabatic potential energy surfaces. *J. Chem. Phys.* **2004**, *121*, 2515–2527.
- (71) Nangia, S.; Truhlar, D. G. Direct calculation of coupled diabatic potential-energy surfaces for ammonia and mapping of a four-dimensional conical intersection seam. *J. Chem. Phys.* **2006**, *124*, 124309.
- (72) Zhu, X.; Yarkony, D. R. Quasi-diabatic representations of adiabatic potential energy surfaces coupled by conical intersections including bond breaking: A more general construction procedure and an analysis of the diabatic representation. *J. Chem. Phys.* **2012**, *137*, 22A511.
- (73) Xie, C.; Zhu, X.; Yarkony, D. R.; Guo, H. Permutation invariant polynomial neural network approach to fitting potential energy surfaces. IV. Coupled diabatic potential energy matrices. *J. Chem. Phys.* **2018**, *149*, 144107.
- (74) Guan, Y.; Guo, H.; Yarkony, D. R. Neural network based quasi-diabatic Hamiltonians with symmetry adaptation and a correct description of conical intersections. *J. Chem. Phys.* **2019**, *150*, 214101.
- (75) Lenzen, T.; Eisfeld, W.; Manthe, U. Vibronically and spin-orbit coupled diabatic potentials for  $X(^2P) + CH_4 \rightarrow HX + CH_3$  reactions: Neural network potentials for  $X = Cl$ . *J. Chem. Phys.* **2019**, *150*, 244115.
- (76) Welsch, R.; Huarte-Larrañaga, F.; Manthe, U. State-to-state reaction probabilities within the quantum transition state framework. *J. Chem. Phys.* **2012**, *136*, 064117.
- (77) Manthe, U.; Welsch, R. Correlation functions for fully or partially state-resolved reactive scattering calculations. *J. Chem. Phys.* **2014**, *140*, 244113.
- (78) Zhao, H.; Umer, U.; Hu, X.; Xie, D.; Sun, Z. An interaction-asymptotic region decomposition method for general state-to-state reactive scatterings. *J. Chem. Phys.* **2019**, *150*, 134105.

- (79) Zhao, B.; Manthe, U. Counter-propagating wave packets in the quantum transition state approach to reactive scattering. *J. Chem. Phys.* **2019**, *150*, 184103.
- (80) Zhao, H. L.; Hu, X. X.; Xie, D. Q.; Sun, Z. G. Quantum wavepacket method for state-to-state reactive cross sections in hyperspherical coordinates. *J. Chem. Phys.* **2018**, *149*, 174103.
- (81) Huang, J.; Liu, S.; Zhang, D. H.; Krems, R. V. Time-dependent wave packet dynamics calculations of cross sections for ultracold scattering of molecules. *Phys. Rev. Lett.* **2018**, *120*, 143401.
- (82) Huang, Y.; Zhao, H.-L.; Usman, S. K.; Ajibade, G. A.; Sun, Z.-g. High-accurate transparent boundary conditions for time-dependent quantum wave packet method. *Chin. J. Chem. Phys.* **2020**, *33*, 258–262.
- (83) Light, J. C.; Carrington, T., Jr. Discrete-variable representations and their utilization. *Adv. Chem. Phys.* **2007**, *114*, 263–310.
- (84) Zhang, Z.; Gatti, F.; Zhang, D. H. Full dimensional quantum mechanical calculations of the reaction probability of the H + NH<sub>3</sub> collision based on a mixed Jacobi and Radau description. *J. Chem. Phys.* **2019**, *150*, 204301.
- (85) Zhang, Z.; Gatti, F.; Zhang, D. H. Full-dimensional quantum mechanical calculations of the reaction probability of the H + CH<sub>4</sub> reaction based on a mixed Jacobi and Radau description. *J. Chem. Phys.* **2020**, *152*, 201101.
- (86) Schapers, D.; Zhao, B.; Manthe, U. Coordinate systems and kinetic energy operators for multi-configurational time-dependent Hartree calculations studying reactions of methane. *Chem. Phys.* **2018**, *509*, 37–44.
- (87) Welsch, R.; Manthe, U. Full-dimensional and reduced-dimensional calculations of initial state-selected reaction probabilities studying the H + CH<sub>4</sub> → H<sub>2</sub> + CH<sub>3</sub> reaction on a neural network PES. *J. Chem. Phys.* **2015**, *142*, 064309.
- (88) Welsch, R.; Manthe, U. Loss of memory in H + CH<sub>4</sub> → H<sub>2</sub> + CH<sub>3</sub> state-to-state reactive scattering. *J. Phys. Chem. Lett.* **2015**, *6*, 338–342.
- (89) Ellerbrock, R.; Manthe, U. Communication: Reactivity borrowing in the mode selective chemistry of H + CHD<sub>3</sub> → H<sub>2</sub> + CD<sub>3</sub>. *J. Chem. Phys.* **2017**, *147*, 241104.
- (90) Ellerbrock, R.; Manthe, U. Full-dimensional quantum dynamics calculations for H + CHD<sub>3</sub>, H<sub>2</sub> + CD<sub>3</sub>: The effect of multiple vibrational excitations. *J. Chem. Phys.* **2018**, *148*, 224303.
- (91) Ellerbrock, R.; Manthe, U. Natural reaction channels in H + CHD<sub>3</sub> → H<sub>2</sub> + CD<sub>3</sub>. *Faraday Discuss.* **2018**, *212*, 217–235.
- (92) Schäpers, D.; Manthe, U. Quasi-bound states of the F-CH<sub>4</sub> complex. *J. Phys. Chem. A* **2016**, *120*, 3186–3195.
- (93) Schäpers, D.; Manthe, U. Vibronic coupling in the F-CH<sub>4</sub> prereactive complex. *J. Chem. Phys.* **2019**, *151*, 104106.
- (94) Zhao, B.; Manthe, U. A transition-state based rotational sudden (TSRS) approximation for polyatomic reactive scattering. *J. Chem. Phys.* **2017**, *147*, 144104.
- (95) Chen, Z.; Chen, J.; Chen, R.; Xie, T.; Wang, X.; Liu, S.; Wu, G.; Dai, D.; Yang, X.; Zhang, D. H. Reactivity oscillation in the heavy-light-heavy Cl + CH<sub>4</sub> reaction. *Proc. Natl. Acad. Sci. U. S. A.* **2020**, *117*, 9202.
- (96) Palma, J.; Clary, D. C. A quantum model Hamiltonian to treat reactions of the type X + YCZ<sub>3</sub> → XY + CZ<sub>3</sub>: Application to O(<sup>3</sup>P) + CH<sub>4</sub> → OH + CH<sub>3</sub>. *J. Chem. Phys.* **2000**, *112*, 1859–1867.
- (97) Zhao, B.; Manthe, U. State-to-state reactive scattering for X + YCZ<sub>3</sub> ⇌ XY + CZ<sub>3</sub> reactions: Eight-dimensional wave packet dynamics within the quantum transition-state framework. *J. Phys. Chem. A*, submitted.
- (98) Manthe, U.; Ellerbrock, R. S-matrix decomposition, natural reaction channels, and the quantum transition state approach to reactive scattering. *J. Chem. Phys.* **2016**, *144*, 204119.
- (99) Hase, W. L. Classical trajectory simulations: Initial conditions. In *Encyclopedia of Computational Chemistry*; Alinger, N. L., Ed.; Wiley: New York, 1998; Vol. 1, pp 399–402.
- (100) Nagy, T.; Lendvay, G. Adiabatic Switching Extended To Prepare Semiclassically Quantized Rotational-Vibrational Initial States for Quasiclassical Trajectory Calculations. *J. Phys. Chem. Lett.* **2017**, *8*, 4621–4626.
- (101) Conte, R.; Parma, L.; Aieta, C.; Rognoni, A.; Ceotto, M. Improved semiclassical dynamics through adiabatic switching trajectory sampling. *J. Chem. Phys.* **2019**, *151*, 214107.
- (102) Bonnet, L. Classical dynamics of chemical reactions in a quantum spirit. *Int. Rev. Phys. Chem.* **2013**, *32*, 171–228.
- (103) Czako, G.; Bowman, J. M. Quasiclassical trajectory calculations of correlated product distributions for the F + CHD<sub>3</sub>(v<sub>1</sub> = 0,1) reactions using an ab initio potential energy surface. *J. Chem. Phys.* **2009**, *131*, 244302.
- (104) Bonnet, L.; Espinosa-Garcia, J. The method of Gaussian weighted trajectories. V. On the 1GB procedure for polyatomic processes. *J. Chem. Phys.* **2010**, *133*, 164108.
- (105) Lee, K. L. K.; Quinn, M. S.; Kolmann, S. J.; Kable, S. H.; Jordan, M. J. T. Zero-point energy conservation in classical trajectory simulations: Application to H<sub>2</sub>CO. *J. Chem. Phys.* **2018**, *148*, 194113.
- (106) Habershon, S.; Manolopoulos, D. E.; Markland, T. E.; Miller, T. F., III Ring-polymer molecular dynamics: Quantum effects in chemical dynamics from classical trajectories in an extended phase space. *Annu. Rev. Phys. Chem.* **2013**, *64*, 387–413.
- (107) Craig, I. R.; Manolopoulos, D. E. Quantum statistics and classical mechanics: Real time correlation function from ring polymer molecular dynamics. *J. Chem. Phys.* **2004**, *121*, 3368–3373.
- (108) Craig, I. R.; Manolopoulos, D. E. Chemical reaction rates from ring polymer molecular dynamics. *J. Chem. Phys.* **2005**, *122*, 084106.
- (109) Suleimanov, Y. V.; Aoiz, F. J.; Guo, H. Chemical reaction rate coefficients from ring polymer molecular dynamics: Theory and practical applications. *J. Phys. Chem. A* **2016**, *120*, 8488–8502.
- (110) Lawrence, J. E.; Manolopoulos, D. E. Path integral methods for reaction rates in complex systems. *Faraday Discuss.* **2020**, *221*, 9–29.
- (111) Suleimanov, Y. V.; Aguado, A.; Gómez-Carrasco, S.; Roncero, O. A ring polymer molecular dynamics approach to study the transition between statistical and direct mechanisms in the H<sub>2</sub> + H<sub>3</sub><sup>+</sup> → H<sub>3</sub><sup>+</sup> + H<sub>2</sub> reaction. *J. Phys. Chem. Lett.* **2018**, *9*, 2133–2137.
- (112) Liu, Q.; Zhang, L.; Li, Y.; Jiang, B. Ring polymer molecular dynamics in gas-surface reactions: Inclusion of quantum effects made simple. *J. Phys. Chem. Lett.* **2019**, *10*, 7475–7481.
- (113) Marjollet, A.; Welsch, R. Nuclear quantum effects in state-selective scattering from ring polymer molecular dynamics. *J. Chem. Phys.* **2020**, *152*, 194113.
- (114) Crim, F. F. Vibrational state control of bimolecular reactions: Discovering and directing the chemistry. *Acc. Chem. Res.* **1999**, *32*, 877–884.
- (115) Polanyi, J. C. Concepts in reaction dynamics. *Acc. Chem. Res.* **1972**, *5*, 161–168.
- (116) Jiang, B.; Guo, H. Relative efficacy of vibrational vs. translational excitation in promoting atom-diatom reactivity: Rigorous examination of Polanyi's rules and proposition of sudden vector projection (SVP) model. *J. Chem. Phys.* **2013**, *138*, 234104.
- (117) Guo, H.; Liu, K. Control of chemical reactivity by transition state and beyond. *Chem. Sci.* **2016**, *7*, 3992–4003.
- (118) Song, H.; Yang, M.; Guo, H. Communication: Equivalence between symmetric and antisymmetric stretching modes of NH<sub>3</sub> in promoting H + NH<sub>3</sub> → H<sub>2</sub> + NH<sub>2</sub> reaction. *J. Chem. Phys.* **2016**, *145*, 131101.
- (119) Qi, J.; Song, H.; Yang, M.; Palma, J.; Manthe, U.; Guo, H. Communication: Mode specific quantum dynamics of the F + CHD<sub>3</sub> → HF + CD<sub>3</sub> reaction. *J. Chem. Phys.* **2016**, *144*, 171101.
- (120) Song, H.; Lu, Y.; Li, J.; Yang, M.; Guo, H. Mode specificity in the OH + CHD<sub>3</sub> reaction: Reduced-dimensional quantum and quasi-classical studies on an ab initio based full-dimensional potential energy surface. *J. Chem. Phys.* **2016**, *144*, 164303.
- (121) Stei, M.; Carrascosa, E.; Dörfler, A.; Meyer, J.; Olsz, B.; Czako, G.; Li, A.; Guo, H.; Wester, R. Stretching vibration is a spectator in nucleophilic substitution. *Sci. Adv.* **2018**, *4*, No. eaas9544.
- (122) Olsz, B.; Czako, G. Mode-specific quasiclassical dynamics of the F<sup>-</sup> + CH<sub>3</sub>I S<sub>N</sub>2 and proton-transfer reactions. *J. Phys. Chem. A* **2018**, *122*, 8143–8151.

- (123) Song, H.; Yang, M. Understanding mode-specific dynamics in the local mode representation. *Phys. Chem. Chem. Phys.* **2018**, *20*, 19647–19655.
- (124) Zhu, Y.; Ping, L.; Bai, M.; Liu, Y.; Song, H.; Li, J.; Yang, M. Tracking the energy flow in the hydrogen exchange reaction  $\text{OH} + \text{H}_2\text{O} \rightarrow \text{H}_2\text{O} + \text{OH}$ . *Phys. Chem. Chem. Phys.* **2018**, *20*, 12543–12556.
- (125) Zheng, R.; Zhu, Y.; Song, H. Mode-specific quantum dynamics and kinetics of the hydrogen abstraction reaction  $\text{OH} + \text{H}_2\text{O} \rightarrow \text{H}_2\text{O} + \text{OH}$ . *Phys. Chem. Chem. Phys.* **2019**, *21*, 24054–24060.
- (126) Corchado, J. C.; Chamorro, M. G.; Rangel, C.; Espinosa-Garcia, J. State-to-state dynamics of the  $\text{Cl}(^2\text{P}) + \text{C}_2\text{H}_6(\nu_5, \nu_1 = 0, 1) \rightarrow \text{HCl}(\nu', j') + \text{C}_2\text{H}_5$  hydrogen abstraction reactions. *Theor. Chem. Acc.* **2019**, *138*, 26.
- (127) Liu, Y.; Song, H.; Xie, D.; Li, J.; Guo, H. Mode specificity in the  $\text{OH} + \text{HO}_2 \rightarrow \text{H}_2\text{O} + \text{O}_2$  reaction: Enhancement of reactivity by exciting a spectator mode. *J. Am. Chem. Soc.* **2020**, *142*, 3331–3335.
- (128) Jiang, B.; Guo, H. Control of mode/bond selectivity and product energy disposal by the transition state: The  $\text{X} + \text{H}_2\text{O}$  ( $\text{X} = \text{H}, \text{F}, \text{O}(^3\text{P})$ , and  $\text{Cl}$ ) reactions. *J. Am. Chem. Soc.* **2013**, *135*, 15251–15256.
- (129) Jiang, B.; Guo, H. Mode specificity, bond selectivity, and product energy disposal in  $\text{X} + \text{CH}_4/\text{CHD}_3$  ( $\text{X} = \text{H}, \text{F}, \text{O}(^3\text{P})$ ,  $\text{Cl}$ , and  $\text{OH}$ ) hydrogen abstraction reactions: Perspective from sudden vector projection model. *J. Chin. Chem. Soc.* **2014**, *61*, 847–859.
- (130) Rivero, U.; Unke, O. T.; Meuwly, M.; Willitsch, S. Reactive atomistic simulations of Diels-Alder reactions: The importance of molecular rotations. *J. Chem. Phys.* **2019**, *151*, 104301.
- (131) Li, A.; Guo, H. Prediction of mode specificity in 1,3-dipolar cycloadditions using the Sudden Vector Projection model. *Chem. Phys. Lett.* **2015**, *624*, 102–106.
- (132) Liu, Y.; Li, J. Quantitative dynamics of the  $\text{N}_2\text{O} + \text{C}_2\text{H}_2 \rightarrow$  oxadiazole reaction: A model for 1,3-dipolar cycloadditions. *ACS Omega* **2020**, *5*, 23343–23350.
- (133) Welsch, R.; Manthe, U. Communication: Ro-vibrational control of chemical reactivity in  $\text{H} + \text{CH}_4 \rightarrow \text{H}_2 + \text{CH}_3$ : Full-dimensional quantum dynamics calculations and a sudden model. *J. Chem. Phys.* **2014**, *141*, 051102.
- (134) Wang, Y.; Song, H.; Szabó, I.; Czakó, G.; Guo, H.; Yang, M. Mode-specific  $\text{S}_{\text{N}}2$  reaction dynamics. *J. Phys. Chem. Lett.* **2016**, *7*, 3322–3327.
- (135) Rangel, C.; Espinosa-Garcia, J. Full-dimensional analytical potential energy surface describing the gas-phase  $\text{Cl} + \text{C}_2\text{H}_6$  reaction and kinetics study of rate constants and kinetic isotope effects. *Phys. Chem. Chem. Phys.* **2018**, *20*, 3925–3938.
- (136) Espinosa-Garcia, J.; Corchado, J. C.; Garcia-Chamorro, M.; Rangel, C.  $\text{F}(^2\text{P}) + \text{C}_2\text{H}_6 \rightarrow \text{HF} + \text{C}_2\text{H}_5$  kinetics study based on a new analytical potential energy surface. *Phys. Chem. Chem. Phys.* **2018**, *20*, 19860–19870.
- (137) Espinosa-Garcia, J.; Garcia-Chamorro, M.; Corchado, J. C. The hydrogen abstraction reaction  $\text{H} + \text{C}_2\text{H}_6 \rightarrow \text{H}_2(\nu, j) + \text{C}_2\text{H}_5$ . Part I. A full-dimensional analytical potential energy surface based on ab initio calculations. *Phys. Chem. Chem. Phys.* **2019**, *21*, 13347–13355.
- (138) Espinosa-Garcia, J.; Garcia-Chamorro, M. Role of an ethyl radical and the problem of  $\text{HF}(\nu)$  bimodal vibrational distribution in the  $\text{F}(^2\text{P}) + \text{C}_2\text{H}_6 \rightarrow \text{HF}(\nu) + \text{C}_2\text{H}_5$  reaction. *Phys. Chem. Chem. Phys.* **2018**, *20*, 26634–26642.
- (139) Espinosa-Garcia, J.; Martinez-Nuñez, E.; Rangel, C. Quasi-classical trajectory dynamics study of the  $\text{Cl}(^2\text{P}) + \text{C}_2\text{H}_6 \rightarrow \text{HCl}(\nu, j) + \text{C}_2\text{H}_5$  reaction. Comparison with experiment. *J. Phys. Chem. A* **2018**, *122*, 2626–2633.
- (140) Espinosa-Garcia, J.; Corchado, J. C. The hydrogen abstraction reaction  $\text{H} + \text{C}_2\text{H}_6 \rightarrow \text{H}_2(\nu, j) + \text{C}_2\text{H}_5$ . Part II. Theoretical kinetics and dynamics study. *Phys. Chem. Chem. Phys.* **2019**, *21*, 13356–13367.
- (141) Rangel, C.; Garcia-Chamorro, M.; Corchado, J. C.; Espinosa-Garcia, J. Kinetics and dynamics study of the  $\text{OH} + \text{C}_2\text{H}_6 \rightarrow \text{H}_2\text{O} + \text{C}_2\text{H}_5$  reaction based on an analytical global potential energy surface. *Phys. Chem. Chem. Phys.* **2020**, *22*, 14796–14810.
- (142) Continetti, R. E.; Guo, H. Dynamics of transient species in polyatomic photodetachment. *Chem. Soc. Rev.* **2017**, *46*, 7650–7667.
- (143) Weichman, M. L.; Neumark, D. M. Slow photoelectron velocity-map imaging of cryogenically cooled anions. *Annu. Rev. Phys. Chem.* **2018**, *69*, 101–124.
- (144) Schatz, G. C. Reaction Dynamics - Detecting resonances. *Science* **2000**, *288*, 1599–1600.
- (145) Yang, T.; Huang, L.; Xiao, C.; Chen, J.; Wang, T.; Dai, D.; Lique, F.; Alexander, M. H.; Sun, Z.; Zhang, D. H.; et al. Enhanced reactivity of fluorine with para-hydrogen in cold interstellar clouds by resonance-induced quantum tunnelling. *Nat. Chem.* **2019**, *11*, 744–749.
- (146) Wang, X.; Dong, W.; Qiu, M.; Ren, Z.; Che, L.; Dai, D.; Wang, X.; Yang, X.; Sun, Z.; Fu, B.; et al.  $\text{HF}(\nu' = 3)$  forward scattering in the  $\text{F} + \text{H}_2$  reaction: Shape resonance and slow-down mechanism. *Proc. Natl. Acad. Sci. U. S. A.* **2008**, *105*, 6227–6231.
- (147) Yang, T.; Chen, J.; Huang, L.; Wang, T.; Xiao, C.; Sun, Z.; Dai, D.; Yang, X.; Zhang, D. H. Extremely short-lived reaction resonances in  $\text{Cl} + \text{HD}(\nu = 1) \rightarrow \text{DCl} + \text{H}$  due to chemical bond softening. *Science* **2015**, *347*, 60–63.
- (148) Otto, R.; Ma, J.; Ray, A. W.; Daluz, J. S.; Li, J.; Guo, H.; Continetti, R. E. Imaging dynamics on the  $\text{F} + \text{H}_2\text{O} \rightarrow \text{HF} + \text{OH}$  potential energy surfaces from wells to barriers. *Science* **2014**, *343*, 396–399.
- (149) Ray, A. W.; Agarwal, J.; Shen, B. B.; Schaefer, H. F.; Continetti, R. E. Energetics and transition-state dynamics of the  $\text{F} + \text{HOCH}_3 \rightarrow \text{HF} + \text{OCH}_3$  reaction. *Phys. Chem. Chem. Phys.* **2016**, *18*, 30612–30621.
- (150) Ray, A. W.; Ma, J.; Otto, R.; Li, J.; Guo, H.; Continetti, R. E. Effects of vibrational excitation on the  $\text{F} + \text{H}_2\text{O} \rightarrow \text{HF} + \text{OH}$  reaction: Dissociative photodetachment of overtone-excited  $[\text{F}-\text{H}-\text{OH}]^-$ . *Chem. Sci.* **2017**, *8*, 7821–7833.
- (151) Ma, J.; Guo, H. Reactive and nonreactive Feshbach resonances accessed by photodetachment of  $\text{FH}_2\text{O}^-$ . *J. Phys. Chem. Lett.* **2015**, *6*, 4822–4826.
- (152) Guo, L.; Li, J.; Ma, J.; Guo, H. Quantum dynamical investigation of product state distributions of the  $\text{F} + \text{CH}_3\text{OH} \rightarrow \text{HF} + \text{CH}_3\text{O}$  reaction via photodetachment of the  $\text{F}^-(\text{HOCH}_3)$  anion. *J. Chem. Phys.* **2019**, *150*, 044301.
- (153) Zhao, B.; Guo, H. Modulations of transition-state control of state-to-state dynamics in the  $\text{F} + \text{H}_2\text{O} \rightarrow \text{HF} + \text{OH}$  reaction. *J. Phys. Chem. Lett.* **2015**, *6*, 676–680.
- (154) Zhang, X.; Li, L.; Chen, J.; Liu, S.; Zhang, D. H. Feshbach resonances in the  $\text{F} + \text{H}_2\text{O} \rightarrow \text{HF} + \text{OH}$  reaction. *Nat. Commun.* **2020**, *11*, 223.
- (155) Westermann, T.; Eisfeld, W.; Manthe, U. Coupled potential energy surface for the  $\text{F}(^2\text{P}) + \text{CH}_4 \rightarrow \text{HF} + \text{CH}_3$  entrance channel and quantum dynamics of the  $\text{CH}_4 \cdot \text{F}^-$  photodetachment. *J. Chem. Phys.* **2013**, *139*, 014309.
- (156) Westermann, T.; Kim, J. B.; Weichman, M. L.; Hock, C.; Yacovitch, T. I.; Palma, J.; Neumark, D. M.; Manthe, U. Resonances in the entrance channel of the elementary chemical reaction of fluorine and methane. *Angew. Chem., Int. Ed.* **2014**, *53*, 1122–1126.
- (157) Lenzen, T.; Manthe, U. Vibronically and spin-orbit coupled diabatic potentials for  $\text{X}(\text{P}) + \text{CH}_4 \rightarrow \text{HX} + \text{CH}_3$  reactions: General theory and application for  $\text{X}(\text{P}) = \text{F}(^2\text{P})$ . *J. Chem. Phys.* **2019**, *150*, 064102.
- (158) Zhao, B.; Manthe, U. Non-adiabatic transitions in the reaction of fluorine with methane. *J. Chem. Phys.* **2020**, *152*, 231102.
- (159) Ren, Z.; Che, L.; Qiu, M.; Wang, X.; Dong, W.; Dai, D.; Wang, X.; Yang, X.; Sun, Z.; Fu, B.; et al. Probing the resonance potential in the  $\text{F}$  atom reaction with hydrogen deuteride with spectroscopic accuracy. *Proc. Natl. Acad. Sci. U. S. A.* **2008**, *105*, 12662–12666.
- (160) Li, J.; Dawes, R.; Guo, H. An ab initio based full-dimensional global potential energy surface for  $\text{FH}_2\text{O}(\text{X}^2\text{A}')$  and dynamics for the  $\text{F} + \text{H}_2\text{O} \rightarrow \text{HF} + \text{HO}$  reaction. *J. Chem. Phys.* **2012**, *137*, 094304.
- (161) Li, J.; Guo, H. Quasi-classical trajectory study of the  $\text{F} + \text{H}_2\text{O} \rightarrow \text{HF} + \text{OH}$  reaction: Influence of barrier height, reactant rotational excitation, and isotopic substitution. *Chin. J. Chem. Phys.* **2013**, *26*, 627–634.

- (162) Nguyen, T. L.; Li, J.; Dawes, R.; Stanton, J. F.; Guo, H. Accurate determination of barrier height and kinetics for the  $F + H_2O \rightarrow HF + OH$  reaction. *J. Phys. Chem. A* **2013**, *117*, 8864–8872.
- (163) Czako, G.; Shepler, B. C.; Braams, B. J.; Bowman, J. M. Accurate ab initio potential energy surface, dynamics, and thermochemistry of the  $F + CH_4 \rightarrow HF + CH_3$  reaction. *J. Chem. Phys.* **2009**, *130*, 084301.
- (164) Palma, J.; Manthe, U. A quasiclassical study of the  $F(^2P) + CHD_3$  ( $\nu_1 = 0,1$ ) reactive system on an accurate potential energy surface. *J. Phys. Chem. A* **2015**, *119*, 12209–12217.
- (165) Chen, J.; Xu, X.; Liu, S.; Zhang, D. H. A neural network potential energy surface for the  $F + CH_4$  reaction including multiple channels based on coupled cluster theory. *Phys. Chem. Chem. Phys.* **2018**, *20*, 9090–9100.
- (166) Suits, A. G. Roaming atoms and radicals: A new mechanism in molecular dissociation. *Acc. Chem. Res.* **2008**, *41*, 873–881.
- (167) Bowman, J. M.; Shepler, B. C. Roaming radicals. *Annu. Rev. Phys. Chem.* **2011**, *62*, 531–553.
- (168) Townsend, D.; Lahankar, S. A.; Lee, S. K.; Chambreau, S. D.; Suits, A. G.; Zhang, X.; Rheinecker, J.; Harding, L. B.; Bowman, J. M. The roaming atom: Straying from the reaction path in formaldehyde decomposition. *Science* **2004**, *306*, 1158–1161.
- (169) Suits, A. G. Roaming reactions and dynamics in the van der Waals region. *Annu. Rev. Phys. Chem.* **2020**, *71*, 77–100.
- (170) Christoffel, K. M.; Bowman, J. M. Three reaction pathways in the  $H$  plus  $HCO \rightarrow H_2 + CO$  Reaction. *J. Phys. Chem. A* **2009**, *113*, 4138–4144.
- (171) Takayanagi, T.; Tanaka, T. Roaming dynamics in the  $MgH + H \rightarrow Mg + H_2$  reaction: Quantum dynamics calculations. *Chem. Phys. Lett.* **2011**, *504*, 130–135.
- (172) Bencsura, A.; Lendvay, G. Bimolecular reactions of vibrationally excited molecules. Roaming atom mechanism at low kinetic energies. *J. Phys. Chem. A* **2012**, *116*, 4445–4456.
- (173) Li, A.; Li, J.; Guo, H. Quantum manifestation of roaming in  $H + MgH \rightarrow Mg + H_2$ : The birth of roaming resonances. *J. Phys. Chem. A* **2013**, *117*, 5052–5060.
- (174) Joalland, B.; Shi, Y.; Kamasah, A.; Suits, A. G.; Mebel, A. M. Roaming dynamics in radical addition-elimination reactions. *Nat. Commun.* **2014**, *5*, 4064.
- (175) Mauguère, F. A. L.; Collins, P.; Stamatiadis, S.; Li, A.; Ezra, G. S.; Farantos, S. C.; Kramer, Z. C.; Carpenter, B. K.; Wiggins, S.; Guo, H. Toward understanding the roaming mechanism in  $H + MgH \rightarrow Mg + HH$  reaction. *J. Phys. Chem. A* **2016**, *120*, 5145–5154.
- (176) Cascarini, F. J. J.; Hornung, B.; Quinn, M. S.; Robertson, P. A.; Orr-Ewing, A. J. Collision energy dependence of the competing mechanisms of reaction of chlorine atoms with propene. *J. Phys. Chem. A* **2019**, *123*, 2679–2686.
- (177) Mauguère, F. A. L.; Collins, P.; Ezra, G. S.; Farantos, S. C.; Wiggins, S. Roaming dynamics in ion–molecule reactions: Phase space reaction pathways and geometrical interpretation. *J. Chem. Phys.* **2014**, *140*, 134112.
- (178) Xie, J.; Hase, W. L. Rethinking the  $S_N2$  reaction. *Science* **2016**, *352*, 32–33.
- (179) Bowman, J. M.; Houston, P. L. Theories and simulations of roaming. *Chem. Soc. Rev.* **2017**, *46*, 7615–7624.
- (180) Ma, Y.-T.; Ma, X.; Li, A.; Guo, H.; Yang, L.; Zhang, J.; Hase, W. L. Potential energy surface stationary points and dynamics of the  $F^- + CH_3I$  double inversion mechanism. *Phys. Chem. Chem. Phys.* **2017**, *19*, 20127–20136.
- (181) Li, J.; Dawes, R.; Guo, H. An accurate multi-channel multi-reference full-dimensional global potential energy surface for the lowest triplet state of  $H_2O_2$ . *Phys. Chem. Chem. Phys.* **2016**, *18*, 29825–29835.
- (182) Lu, D.; Xie, C.; Li, J.; Guo, H. Rate coefficients and branching ratio for multi-channel hydrogen abstractions from  $CH_3OH$  by  $F$ . *Chin. J. Chem. Phys.* **2019**, *32*, 84–88.
- (183) Lu, D.; Li, J.; Guo, H. Stereodynamical control of product branching in multi-channel barrierless hydrogen abstraction of  $CH_3OH$  by  $F$ . *Chem. Sci.* **2019**, *10*, 7994–8001.
- (184) Zhu, Y.; Tian, L.; Song, H.; Yang, M. Kinetic and dynamic studies of the  $H_3^+ + CO \rightarrow H_2 + HCO^+ / HOC^+$  reaction on a high-level ab initio potential energy surface. *J. Chem. Phys.* **2019**, *151*, 054311.
- (185) Quémener, G.; Julienne, P. S. Ultracold molecules under control! *Chem. Rev.* **2012**, *112*, 4949–5011.
- (186) Balakrishnan, N. Perspective: Ultracold molecules and the dawn of cold controlled chemistry. *J. Chem. Phys.* **2016**, *145*, 150901.
- (187) Toscano, J.; Lewandowski, H. J.; Heazlewood, B. R. Cold and controlled chemical reaction dynamics. *Phys. Chem. Chem. Phys.* **2020**, *22*, 9180–9194.
- (188) Tizniti, M.; Le Picard, S. D.; Lique, F.; Berteloite, C.; Canosa, A.; Alexander, M. H.; Sims, I. R. The rate of the  $F + H_2$  reaction at very low temperatures. *Nat. Chem.* **2014**, *6*, 141–145.
- (189) De Fazio, D.; Aquilanti, V.; Cavalli, S. Quantum dynamics and kinetics of the  $F + H_2$  and  $F + D_2$  reactions at low and ultra-low temperatures. *Front. Chem.* **2019**, *7*. DOI: 10.3389/fchem.2019.00328
- (190) Skouteris, D.; Castillo, J. F.; Manolopoulos, D. E. ABC: The CCP6 quantum reactive scattering program. *Comput. Phys. Commun.* **2000**, *133*, 128.
- (191) Ni, K.-K.; Ospelkaus, S.; de Miranda, M. H. G.; Pe'er, A.; Neyenhuis, B.; Zirbel, J. J.; Kotochigova, S.; Julienne, P. S.; Jin, D. S.; Ye, J. A high phase-space-density gas of polar molecules. *Science* **2008**, *322*, 231–235.
- (192) Croft, J. F. E.; Makrides, C.; Li, M.; Petrov, A.; Kendrick, B. K.; Balakrishnan, N.; Kotochigova, S. Universality and chaoticity in ultracold  $K + K^+Rb$  chemical reactions. *Nat. Commun.* **2017**, *8*, 15897.
- (193) Rackham, E. J.; Huarde-Larrañaga, F.; Manolopoulos, D. E. Coupled-channel statistical theory of the  $N(^2D) + H_2$  and  $O(^1D) + H_2$  insertion reactions. *Chem. Phys. Lett.* **2001**, *343*, 356–364.
- (194) Rackham, E. J.; Gonzalez-Lezana, T.; Manolopoulos, D. E. A rigorous test of the statistical model for atom-diatom insertion reactions. *J. Chem. Phys.* **2003**, *119*, 12895–12907.
- (195) Makrides, C.; Hazra, J.; Pradhan, G. B.; Petrov, A.; Kendrick, B. K.; Gonzalez-Lezana, T.; Balakrishnan, N.; Kotochigova, S. Ultracold chemistry with alkali-metal–rare-earth molecules. *Phys. Rev. A: At, Mol, Opt. Phys.* **2015**, *91*, 012708.
- (196) Yang, T.; Li, A.; Chen, G. K.; Xie, C.; Suits, A. G.; Campbell, W. C.; Guo, H.; Hudson, E. R. Optical control of reactions between water and laser-cooled  $Be^+$  ions. *J. Phys. Chem. Lett.* **2018**, *9*, 3555–3560.
- (197) Dörfler, A. D.; Eberle, P.; Koner, D.; Tomza, M.; Meuwly, M.; Willitsch, S. Long-range versus short-range effects in cold molecular ion-neutral collisions. *Nat. Commun.* **2019**, *10*, 5429.
- (198) Ospelkaus, S.; Ni, K.-K.; Wang, D.; de Miranda, M. H. G.; Neyenhuis, B.; Quémener, G.; Julienne, P. S.; Bohn, J. L.; Jin, D. S.; Ye, J. Quantum-state controlled chemical reactions of ultracold potassium-rubidium molecules. *Science* **2010**, *327*, 853–857.
- (199) Hu, M. G.; Liu, Y.; Grimes, D. D.; Lin, Y. W.; Gheorghie, A. H.; Vexiau, R.; Bouloufa-Maafa, N.; Dulieu, O.; Rosenband, T.; Ni, K. K. Direct observation of bimolecular reactions of ultracold  $KRb$  molecules. *Science* **2019**, *366*, 1111–1115.
- (200) Yang, D.; Zuo, J.; Huang, J.; Hu, X.; Dawes, R.; Xie, D.; Guo, H. A global full-dimensional potential energy surface for the  $K_2Rb_2$  complex and its lifetime. *J. Phys. Chem. Lett.* **2020**, *11*, 2605–2610.
- (201) Liu, Y.; Hu, M.-G.; Nichols, M. A.; Grimes, D. D.; Karman, T.; Guo, H.; Ni, K.-K. Photo-excitation of long-lived transient intermediates in ultracold reactions. *Nat. Phys.* **2020**. DOI: 10.1038/s41567-020-0968-8.
- (202) Wang, G.; Quémener, G. Tuning ultracold collisions of excited rotational dipolar molecules. *New J. Phys.* **2015**, *17*, 035015.
- (203) Yang, D.; Huang, J.; Hu, X.; Xie, D.; Guo, H. Statistical quantum mechanical approach to diatom-diatom capture dynamics and application to ultracold  $KRb + KRb$  reaction. *J. Chem. Phys.* **2020**, *152*, 241103.
- (204) Gonzalez-Martinez, M. L.; Bonnet, L.; Larregaray, P.; Rayez, J.-C. Classical treatment of molecular collisions: striking improvement of the description of recoil energy distributions using Gaussian weighted trajectories. *J. Chem. Phys.* **2007**, *126*, 041102.
- (205) Buchachenko, A. A.; Stolyarov, A. V.; Szcześniak, M. M.; Chłasiński, G. Ab initio long-range interaction and adiabatic channel



capture model for ultracold reactions between the KRb molecules. *J. Chem. Phys.* **2012**, *137*, 114305.

(206) Kotochigova, S. Dispersion interactions and reactive collisions of ultracold polar molecules. *New J. Phys.* **2010**, *12*, 073041.

(207) Unke, O. T.; Meuwly, M. Toolkit for the construction of reproducing kernel-based representations of data: Application to multidimensional potential energy surfaces. *J. Chem. Inf. Model.* **2017**, *57*, 1923–1931.

(208) Krems, R. V. Cold controlled chemistry. *Phys. Chem. Chem. Phys.* **2008**, *10*, 4079–4092.

(209) Smith, F. T. Diabatic and adiabatic representations for atomic collision problems. *Phys. Rev.* **1969**, *179*, 111–123.

(210) Mead, C. A. The geometric phase in molecular systems. *Rev. Mod. Phys.* **1992**, *64*, 51–85.

(211) Baer, M. Introduction to the theory of electronic non-adiabatic coupling terms in molecular systems. *Phys. Rep.* **2002**, *358*, 75–142.

(212) Kendrick, B. K. Geometric phase effects in chemical reaction dynamics and molecular spectra. *J. Phys. Chem. A* **2003**, *107*, 6739–6756.

(213) Xie, C.; Malbon, C. L.; Guo, H.; Yarkony, D. R. Up to a sign. The insidious effects of energetically inaccessible conical intersections on unimolecular reactions. *Acc. Chem. Res.* **2019**, *52*, 501–509.

(214) Varandas, A. J. C.; Brown, F. B.; Mead, C. A.; Truhlar, D. G.; Blais, N. C. A double many-body expansion of the two lowest-energy potential surfaces and nonadiabatic coupling for H<sub>3</sub>. *J. Chem. Phys.* **1987**, *86*, 6258–6269.

(215) Mead, C. A.; Truhlar, D. G. On the determination of Born-Oppenheimer nuclear motion wave functions including complications due to conical intersections and identical nuclei. *J. Chem. Phys.* **1979**, *70*, 2284–2296.

(216) Juanes-Marcos, J. C.; Althorpe, S. C.; Wrede, E. Theoretical study of geometric phase effects in the hydrogen-exchange reaction. *Science* **2005**, *309*, 1227–1230.

(217) Yuan, D.; Guan, Y.; Chen, W.; Zhao, H.; Yu, S.; Luo, C.; Tan, Y.; Xie, T.; Wang, X.; Sun, Z.; et al. Observation of the geometric phase effect in the H + HD → H<sub>2</sub> + D reaction. *Science* **2018**, *362*, 1289–1293.

(218) Xie, Y.; Zhao, H.; Wang, Y.; Huang, Y.; Wang, T.; Xu, X.; Xiao, C.; Sun, Z.; Zhang, D. H.; Yang, X. Quantum interference in H + HD → H<sub>2</sub> + D between direct abstraction and roaming insertion pathways. *Science* **2020**, *368*, 767–771.

(219) Kendrick, B. K. Non-adiabatic quantum reactive scattering in hyperspherical coordinates. *J. Chem. Phys.* **2018**, *148*, 044116.

(220) Kendrick, B. K.; Hazra, J.; Balakrishnan, N. The geometric phase controls ultracold chemistry. *Nat. Commun.* **2015**, *6*, 7918.

(221) Kendrick, B. K.; Hazra, J.; Balakrishnan, N. Geometric phase appears in the ultracold hydrogen exchange reaction. *Phys. Rev. Lett.* **2015**, *115*, 153201.

(222) Alexander, M. H.; Manolopoulos, D. E.; Werner, H.-J. An investigation of the F+H<sub>2</sub> reaction based on a full ab initio description of the open-shell character of the F(<sup>2</sup>P) atom. *J. Chem. Phys.* **2000**, *113*, 11084–11100.

(223) Capecchi, G.; Werner, H. J. Ab initio calculations of coupled potential energy surfaces for the Cl(<sup>2</sup>P<sub>3/2</sub>, <sup>2</sup>P<sub>1/2</sub>) + H<sub>2</sub> reaction. *Phys. Chem. Chem. Phys.* **2004**, *6*, 4975–4983.

(224) Palma, J.; Manthe, U. Non-adiabatic effects in F + CHD<sub>3</sub> reactive scattering. *J. Chem. Phys.* **2017**, *146*, 214117.

(225) Ortiz-Suárez, M.; Witinski, M. F.; Davis, H. F. Reactive quenching of OH(A<sup>2</sup>Σ<sup>+</sup>) by D<sub>2</sub> studied using crossed molecular beams. *J. Chem. Phys.* **2006**, *124*, 201106.

(226) Dempsey, L. P.; Murray, C.; Lester, M. I. Product branching between reactive and nonreactive pathways in the collisional quenching of OH A<sup>2</sup>Σ<sup>+</sup> radicals by H<sub>2</sub>. *J. Chem. Phys.* **2007**, *127*, 151101.

(227) Yarkony, D. R. Substituent effects and the noncrossing rule: The importance of reduced symmetry subspaces. I. The quenching of OH(A<sup>2</sup>Σ<sup>+</sup>) by H<sub>2</sub>. *J. Chem. Phys.* **1999**, *111*, 6661–6664.

(228) Hoffman, B. C.; Yarkony, D. R. The role of conical intersections in the nonadiabatic quenching of OH(A<sup>2</sup>Σ<sup>+</sup>) by molecular hydrogen. *J. Chem. Phys.* **2000**, *113*, 10091–10099.

(229) Collins, M. A.; Godsi, O.; Liu, S.; Zhang, D. H. An ab initio quasi-diabatic potential energy matrix for OH(<sup>2</sup>Σ) + H<sub>2</sub>. *J. Chem. Phys.* **2011**, *135*, 234307.

(230) Shu, Y.; Kryven, J.; Sampaio de Oliveira-Filho, A. G.; Zhang, L.; Song, G.-L.; Li, S. L.; Meana-Pañeda, R.; Fu, B.; Bowman, J. M.; Truhlar, D. G. Direct diabaticization and analytic representation of coupled potential energy surfaces and couplings for the reactive quenching of the excited <sup>2</sup>Σ<sup>+</sup> state of OH by molecular hydrogen. *J. Chem. Phys.* **2019**, *151*, 104311.

(231) Malbon, C. L.; Zhao, B.; Guo, H.; Yarkony, D. R. On the nonadiabatic collisional quenching of OH(A) by H<sub>2</sub>: a four coupled quasi-diabatic state description. *Phys. Chem. Chem. Phys.* **2020**, *22*, 13516–13527.

(232) Zhang, P.-Y.; Lu, R.-F.; Chu, T.-S.; Han, K.-L. Quenching of OH(A<sup>2</sup>Σ<sup>+</sup>) by H<sub>2</sub> through conical intersections: Highly excited products in nonreactive channel. *J. Phys. Chem. A* **2010**, *114*, 6565–6568.

(233) Dillon, J.; Yarkony, D. R. Seams of conical intersections relevant to the quenching of OH(A<sup>2</sup>Σ<sup>+</sup>) by collisions with H<sub>2</sub>. *J. Phys. Chem. A* **2013**, *117*, 7344–7355.

(234) Kamarchik, E.; Fu, B.; Bowman, J. M. Communications: Classical trajectory study of the postquenching dynamics of OH A<sup>2</sup>Σ<sup>+</sup> by H<sub>2</sub> initiated at conical intersections. *J. Chem. Phys.* **2010**, *132*, 091102.

(235) Fu, B.; Kamarchik, E.; Bowman, J. M. Quasiclassical trajectory study of the postquenching dynamics of OH A<sup>2</sup>Σ<sup>+</sup> by H<sub>2</sub>/D<sub>2</sub> on a global potential energy surface. *J. Chem. Phys.* **2010**, *133*, 164306.

(236) Li, H.; Suits, A. G. Universal crossed beam imaging studies of polyatomic reaction dynamics. *Phys. Chem. Chem. Phys.* **2020**, *22*, 11126–11138.

(237) De Marco, L.; Valtolina, G.; Matsuda, K.; Tobias, W. G.; Covey, J. P.; Ye, J. A degenerate Fermi gas of polar molecules. *Science* **2019**, *363*, 853–856.